frontiers in Earth Science

ORIGINAL RESEARCH
published: 10 July 2020
doi: 10.3389/feart.2020.00218

Assessing the Dynamics of Dissolved Organic Matter (DOM) in the Coastal Environments Dominated by Mangroves, Indian Sundarbans

Prasun Sanyal[1], Raghab Ray[2], Madhusudan Paul[1], Vandana Kumari Gupta[1], Avanti Acharya[1], Sneha Bakshi[1], Tapan Kumar Jana[1] and Sandip Kumar Mukhopadhyay[1]**

[1] Department of Marine Science, University of Calcutta, Kolkata, India, [2] Department of Chemical Oceanography, Atmosphere and Ocean Research Institute, The University of Tokyo, Kashiwa, Japan

Tidal transport from coastal wetlands ("outwelling"), together with riverine fluxes, provide the most important sources of terrigenous organic matter (OM) to the ocean. The flux of dissolved organic carbon (DOC) from the mangrove swamps accounts for 10% of the terrestrial DOC flux to the coastal water. This study examines the sources, distribution, and export of dissolved OM at interannual, seasonal, and diurnal bases along the estuaries located at the Sundarbans, the world's largest deltaic mangrove and heritage site. Sampling was carried out from the riverine (Hooghly) and mangrove-dominated tidal estuaries (Saptamukhi, Thakuran, Matla), covering all three seasons (pre-monsoon, monsoon, and post-monsoon) during 2012–2017. DOC varied at a broad range, from 109 to 462 μM (n = 146), with higher concentration observed in the Hooghly (383 ± 120 μM, n = 35) than the mangrove estuaries (246 ± 82 to 266 ± 120 μM, n = 111). Non-conservative mixing of DOC along the salinity gradient attested to mangrove input, particularly in the polyhaline waters. Upper and mid estuarine zones of the mangrove estuaries showed slightly higher DOC concentration (270 ± 92 μM, n = 84, salinity range 18–25) than in the mouth (250 ± 85 μM, n = 27, salinity range 26–27), because of the dilution with marine waters having low DOC concentration and shorter water residence time downstream. Seasonally, higher DOC concentration during the post-monsoon might be linked to higher litterfall, promoting leaching of organic compounds to the water. In that connection, colored dissolved organic matter (CDOM) could be a by-product of mangrove litter leaching, and its absorption coefficient (at 350 nm) exhibited non-conservative mixing pattern at wide ranges from 2.5 to 7.6 m^{-1} (n = 40). CDOM enrichment was observed in the surface water during the low tide when outwelling maximized. Overall, the central and eastern parts of the Indian Sundarbans showed enrichment of more terrigenous type CDOM (evident from optical proxies, e.g., $S_{275-295}$ and $SUVA_{254}$) than the western part, probably due to greater mangrove productivity in the eastern side. Flux estimates of DOM resulted in higher yield and export of mangrove-derived DOC but lower export of CDOM to the Bay of Bengal as compared to their riverine transport.

Keywords: dissolved organic matter, CDOM, mangrove, Sundarbans, Hooghly estuary

OPEN ACCESS

Edited by:
Luiz Drude Lacerda, Federal University of Ceará, Brazil

Reviewed by:
Luiz Carlos Cotovicz Jr., Federal University of Ceará, Brazil
Stéphane Jean Louis Mounier, Université de Toulon, France

***Correspondence:**
Raghab Ray
raghab.ray@aori.u-tokyo.ac.jp
Sandip Kumar Mukhopadhyay
skm.caluniv@gmail.com

Specialty section:
This article was submitted to Biogeoscience, a section of the journal Frontiers in Earth Science

Received: *24 May 2019*
Accepted: *25 May 2020*
Published: *10 July 2020*

Citation:
Sanyal P, Ray R, Paul M, Gupta VK, Acharya A, Bakshi S, Jana TK and Mukhopadhyay SK (2020) Assessing the Dynamics of Dissolved Organic Matter (DOM) in the Coastal Environments Dominated by Mangroves, Indian Sundarbans. Front. Earth Sci. 8:218. doi: 10.3389/feart.2020.00218

INTRODUCTION

Dissolved organic carbon (DOC), holding >200 times the carbon inventory of marine biomass (Hansell et al., 2009) is the largest C reservoir in the marine environment, yet is the least understood component of the global C cycle (Hansell and Carlson, 2001). DOC, a major component of dissolved organic matter (DOM) has many implications in ecosystem functions, such as forming complexes with metals (Midorikawa and Tanoue, 1998); absorbing ultraviolet (UV) and visible light and acting as a "sunscreen" to the marine microorganisms, thereby controlling primary production in the upper water column (Arrigo and Brown, 1996); and reacting with free radicals in the media as an antioxidant (Romera-Castillo and Jaffé, 2015). However, the most vital role of DOC is as a food supplement in the marine microbial loop, supporting growth of the microorganisms (Zweifel et al., 1995) and long-term C sequestration in the bottom ocean (Hansell et al., 2009).

In global C cycle, the ocean inventory of DOC is comparable to the mass of inorganic C in the atmosphere (IPCC, 2007). Net oceanic uptake of CO_2 is ∼1.9 Pg C yr^{-1} (1 Pg = 10^{15} g) (Sarmiento and Gruber, 2006); therefore, small perturbation in the processes regulating DOC production and removal in the ocean could influence atmosphere CO_2 balance and OC export with consequences for the climate. It is seen that net oxidation of only 1% of the seawater DOC pool within 1 year could be sufficient to generate a CO_2 flux of 7 Pg C yr^{-1}, being comparable to that produced annually by fossil fuel combustion (Hedges, 2002). A large-scale oxidation of DOC could accelerate temperature rise and deglaciation (Peltier et al., 2007).

Besides primary production in the ocean, DOC originates from land-driven transport via rivers, inland waters, estuaries, and wetlands. Globally, DOC comprises about 22% of the riverine- and estuarine-derived C to the ocean (Bauer and Bianchi, 2011). Another subset of DOM that absorbs UV and visible light is referred to as chromophoric or colored dissolved organic matter (CDOM). In subtropical and tropical coastal waters, mangrove leaf litter (Scully et al., 2004; Maie et al., 2008) is a potentially important source of CDOM, which comprises >10% of the terrestrial organic matter (OM) export to the global ocean (Jennerjahn and Ittekkot, 2002; Dittmar et al., 2006). CDOM is largely responsible in controlling the optical properties of most natural waters. Photochemical reactions involving DOC and CDOM can affect the oxidizing capacity of OM, nutrient dynamics, trace gas exchange, the color of surface waters, and biological activity in the euphotic zone of the ocean (Pelizzetti and Calza, 2002). Very high concentration of CDOM could reduce sunlight penetration into the water, and thus, could limit photosynthesis by inhibiting the growth of primary producers. On other side, CDOM absorbs harmful UVA/B radiation, protecting organisms from DNA damage. Upon UV exposure, CDOM tends to "bleach," producing low-molecular-weight organic compounds, which may be utilized by the microbial communities, releasing nutrients that may be used by the phytoplankton communities as nutrient source, and generating reactive oxygen species that may damage tissues and alter bioavailability of limiting trace metals (Jaffe et al., 2008; Ganju et al., 2014).

Optical measurements of absorbance and fluorescence have been increasingly performed to characterize marine DOM composition and to infer its sources and biogeochemistry (Hansen et al., 2016). Only a subset of DOM has marine waters, and about 50–70% is represented by the CDOM (Coble, 2007). The CDOM in the coastal and marine environments is mainly terrestrially originated from the degradation of upland vegetation via surface run-off and autochthonous physical and biogeochemical processes (Coble, 2007; Shank et al., 2009; Chari et al., 2019). The presence of a mixture of aromatic polymers and proteins (Yamashita and Tanoue, 2009; Fichot et al., 2016), mainly resulting from the decomposition of OM, is responsible to produce humic substances, derived from the vascular and non-vascular plants. CDOM optical descriptors, such as absorption coefficient at 350 nm ($a_{cdom}350$), spectral slopes (S) of the UV absorbance (spectra slope between 275 nm and 295 nm as $S_{275-295}$ and slope ratio in the ranges of 275 to 295 nm and 350 to 400 nm as S_R), and specific UV absorption at 254 nm ($SUVA_{254}$), provide valuable insights into the various characteristics of DOM (Blough and Del Vecchio, 2002; Fichot and Benner, 2011; Lu et al., 2016). Slope has been used for correcting remote sensing (bio-optic) data (Schwartz et al., 2002; Vantrepotte et al., 2015) and monitoring CDOM degradative processes (Helms et al., 2013). $SUVA_{254}$ provides information on the aromaticity and molecular weight of the bulk DOC pool (Weishaar et al., 2003).

Despite recognition of the coastal ecosystems (including estuaries, rivers, and tidal wetlands) as a component of oceanic C cycle in the Fifth International Panel on Climate Change (IPCC, AR5), efforts to elucidate the fate and cycling of DOM in the coastal ocean and its export to the ocean have still been very limited (Lønborg and Álvarez-Salgado, 2012; Raymond and Spencer, 2013; Barrón and Duarte, 2015). The estimation of DOC accumulation in mangrove dominated estuarine systems is challenging due to confounding presence of terrigenous DOC and mangrove-derived DOC, complexities associated with hydrology (annual river discharge, rainfall, and evaporation), tidal regime, topography, wetland productivity, and the inherent molecular and structural complexities within the DOM pool. Among tidal wetlands, mangroves that cover a large area of the coastal margin of tropical and subtropical regions (13.78 million ha; Giri et al., 2014) are even more complex, due to their ability to trap organic particles within the intricate root systems, releasing DOC from pore water via tidal pumping and litter leaching (Bergamaschi et al., 2012; Maher et al., 2013). Mangroves are putatively known for exporting DOC to the adjacent sea (de Rezende et al., 2007; Cawley et al., 2013; Ho et al., 2017; Ray et al., 2018a,b). The contribution of DOC from mangroves is equivalent to 10% of the total global DOC export from rivers to the ocean (Dittmar et al., 2006). About half of the net primary production in mangroves is exported as OM to the ocean (Alongi, 2014). Recently, mangroves have been recognized to contribute ∼ 60% of global exchangeable DOC (EDOC) flux from the ocean to the

atmosphere (Sippo et al., 2017). EDOC consists of volatile and semi-volatile organic compounds, which are ubiquitous C species that play a major role in global tropospheric chemistry (Fuentes et al., 2000). Therefore, it is important to unveil the dynamics of DOM in coastal environments dominated by the mangroves.

BACKGROUND AND OBJECTIVES

The relationships between CDOM and DOC could depend on many factors (Harvey et al., 2015). The role and inter-relationships of DOC and CDOM in the mangrove-dominated estuarine water of the Sundarbans and surrounding coastal areas have not been studied till date. This study considers the Sundarbans, the world's largest deltaic mangroves, at the lower Gangetic delta of the northeast Bay of Bengal (BoB), for developing robust understanding of sources, mixing, and export of DOM.

The Ganges-Brahmaputra estuary is particularly vulnerable to anthropogenic perturbations, due to high nutrient loads from river discharges (Seitzinger et al., 2005; Mukhopadhyay et al., 2006), in part as a result of economic growth in areas reclaimed from mangrove forest. Previously, Indian Sundarbans was recognized as a source of DOC exporting about 3.03 Tg C/year (1 Tg = 10^{12} g, Ray et al., 2018a). However, in that study, sampling stations were chosen only in the western part of the mangroves, which is fed by fresh water from the connecting channel of Hooghly estuary; but the central and eastern regions, having limited freshwater supply, were not considered for water sampling. Dutta et al. (2019) observed higher CO_2 emission from the anthropogenically perturbed Hooghly estuary than the Indian Sundarbans. It is noteworthy that the eastern part of the mangroves was recognized to store more C in its above and below ground biomass (AGB and BGB, respectively) than the western part (Ray et al., 2011). Therefore, an extent of spatial coverage is essential to better estimate DOM yield and associated export/import flux. Furthermore, intensification of the southwest monsoon as a result of global warming could drive future increases of freshwater flux, OM, and nutrient input (Biswas et al., 2010). Previously, DOC flux from the Sundarbans and Hooghly estuary was estimated based on pre-monsoon and post-monsoon observations (Ray et al., 2015, 2018a); but in our present work, DOM flux is revisited, considering monsoonal changes as well. Leaf litter leaching from vascular mangrove plants could be a major source of CDOM to the coastal ocean waters of the Indian Sundarbans, where some of highest litter fall rates were recorded by Ray et al. (2011). We hypothesize that the presence of dense mangroves alongside the deltaic coastlines of the BoB would mainly control estuarine DOM biogeochemistry.

Therefore, present research conducted in the Indian Sundarbans aims (1) to resolve spatio-temporal variability of the DOM distribution pattern along the estuarine transects, (2) to characterize DOM sources and their transformation during the transport, and (3) to examine the relationship between DOC and CDOM loads and quantify their export rates to the BoB.

MATERIALS AND METHODS

Study Area, Waterways, Soil, and Climate

The Indian Sundarbans ecosystem (∼9,600 km^2) is situated at the land–ocean boundary of the Ganges-Brahmaputra delta and BoB (20°32–20°40 N, 88°05–89° E). The Sundarbans, a world heritage site and a highly bio-diversified ecoregion, is the largest monsoonal, macro-tidal delta-front of the estuarine system in India and Bangladesh. The Indian part of the Sundarbans covers 4,264 km^2 as dense mangroves forest, and 1,781 km^2 as aquatic ecosystem (Ray et al., 2018a). The main artery of this ecosystem, the river Ganges along with its several distributaries, meets in the BoB, forming India's largest estuarine complex. The lower part of this estuarine system is a complex network of numerous creeks, distributaries, and several marshy islands (Ray et al., 2011; Chatterjee et al., 2013). Due to gentle slope of the coast and large tidal amplitude, water penetrates at an average distance of 110 km inland from the shoreline, the effect of which could be felt over 300 km inland. Most of the rivers in the Sundarbans flow north to south and are influenced by the tides coming from the BoB. The channels connecting these rivers generally flow east or west. Silt-laden rivers, rivulets, and creeks are abundant across the Sundarbans. The main estuaries from west to east are Hooghly, Muriganga, Saptamukhi, Thakuran, Matla, Bidyadhari, Gosaba, and Harinbahnaga. These estuaries, apart from the Hooghly, have no connection with the Ganges. The Hooghly, an approximately 260-km-long distributary of the Ganges river, is the main artery of the Indian Sundarbans and is influenced by freshwater discharge from Farrakka dam, located 285 km upstream from the mouth of the estuary. The Hooghly estuary bifurcates into the Hooghly main channel before its meeting with the BoB, and the other part is connected to the Saptamukhi estuary via Hatani-Duani channel as a source of freshwater to the mangroves (Ray et al., 2015). The inner estuaries of the Indian Sundarbans that also cover our water-sampling points are smaller in length than the Hooghly (Saptamukhi west: 41 km, Saptamukhi east: 64 km, Thakuran: 62 km, and Matla: 125 km; Sanyal, 1983; Chatterjee et al., 2013), maintained by the semi-diurnal tides at their mouths and limited freshwater received as local runoff.

In the Sundarbans, the fine-grained muddy sediment with moderate organic C (silty clay ∼ 90%, OC ∼ 0.65%; Ray et al., 2011) and nutrient conditions (carbon-use efficiency of 0.86–1.0 for sediment with C:N ratios of 10–13; Ray et al., 2017) favors the dominance of mangrove species like *Avicennia alba*, *Avicennia marina*, *Avicennia officinalis*, *Sonneratia apetala*, *Ceriops decandra*, *Aegialitis rotundifolia*, *Bruguiera gynorrhiza*, *Heriteira fomes*, etc. Maximum mangrove litterfall was observed in winter or in the post-monsoon (about 100–300 g dry weight m^{-2} $month^{-1}$, Ray et al., 2011).

The seasonal climate is generally categorized into pre-monsoon (March to June), monsoon (July to October), and post-monsoon (November to February). Progressive increase of

temperature and rainfall occur during the pre-monsoon and monsoon respectively, with temperatures ranging between 12°C and 34°C and rainfall between 0 to 461 mm. In the monsoon periods, maximum freshwater discharge from the Hooghly river estuary was recorded by Rudra (2014), with annual ranges between 1,113 and 6,416 $m^3\ s^{-1}$.

Sampling Procedure and Chemical Analysis

In total, 10 field campaigns were conducted during 2012–2017. Collections of dissolved and suspended particulate samples were performed from four major estuaries of the Hooghly Sundarbans mangrove ecosystem [i.e., Hooghly (H), Saptamukhi (S), Thakuran (T), and Matla (M)], covering all three seasons (pre-monsoon, monsoon, and post-monsoon). Surface water and bottom water were sampled from the longitudinal transects of the estuaries, being classified as upper, middle, and lower stretches (Hooghly upper, middle, and lower as HU, HM, and HL, respectively; Saptamukhi upper, middle and lower: SU, SM, and SL, respectively; Thakuran upper, middle, and lower: TU, TM, and TL, respectively; and Matla upper, middle, and lower: MU, MM, and ML, respectively). It was necessary to sample both surface and bottom water for examining the water column profile of DOM in the estuaries that are fed by river water from the Hooghly upstream; thus, the existence of halocline could be a probable phenomenon there. However, due to logistical reasons, we could only collect bottom water samples occasionally. Sampling was performed primarily based on the prominent salinity gradient (ranging 0 to 28) in the Hooghly. For the mangrove estuaries, such a distinct salinity gradient was absent; instead, longitudinal sampling along the estuaries was conducted. Among the DOM parameters, DOC was the main component collected during all 10 expeditions, while surface water samples for CDOM optical parameters were collected from 3 expeditions, covering all three seasons for the S, T, and M series (post-monsoon 2016, monsoon 2017, and pre-monsoon 2017), and one season for the H series (post-monsoon 2016). Already-acquired and published results on DOC and isotopic compositions (δ^{13}DOC) from the Hooghly and Saptamukhi estuary in 2014 were used for compilation (Ray et al., 2015, 2018a). Time series observations of 20 h and 24 h were performed at SM in 2014 (December 28–31; published data by Ray et al., 2015) and 2017 (March 29–30; present work), respectively. However, in the subsequent discussion, we will explain mainly the results of the 24-h time series observation. DOC was collected in both surveys at hourly basis, while CDOM was collected at bi-hourly basis only in 2017. The SM site was located close to a mangrove creek of Lothian Island (38 $km^{2)}$, which is situated at confluence of the Saptamukhi estuary and the BoB, meaning in the buffer zone of the Sundarbans Biosphere Reserve (station 1, 21°32′–21°40′N and 88°05′–89°E). The tectonic setting, geographic location, and species richness made Lothian Island an ideal representative of a more or less pristine mangrove forest within the Sundarbans (Ray et al., 2015). Data on daily tidal amplitude from a gauge station near Hooghly downstream (Sagar Island) were provided by the Kolkata Port Trust, West Bengal. For more details on water sampling performances and measured parameters, refer to **Table 1**.

Discrete water samples were collected using Niskin water sampler (5-L capacity; Oceantest Equipment Inc.) for both surface and bottom water (refers to map in **Figure 1**). Water temperature was recorded by thermometer. Salinity and dissolved oxygen (DO) were measured on-board following Mohr-Knudsen and Winkler titration, respectively (Grasshoff, 1983). Samples for total suspended matter (TSM) and dissolved nutrients were collected in 1-L acid-cleaned amber HDPE bottles and were stored in a cool box before filtration of a known volume of water on pre-weighed 47 mm/0.7 μm Whatman GF/F filters. Filtrates were stored in a cool box on ice during transportation to the laboratory. Residue was washed with MilliQ water, and TSM content was determined by drying the filter paper at 60°C to a constant weight. Simultaneously, for chlorophyll-a (Chl-a), 1 L of water samples were collected in amber HDPE bottles and filtered under a low-light condition through 47-mm Whatman GF/F filters (pore size, 0.7 μm). Wet filters were kept in cryovials and stored in liquid nitrogen till further analyses. For bulk measurement of DOC and δ^{13}DOC, water samples were directly filtered using a glass syringe and pre-combusted (overnight at 450^{o}C) 25-mm Whatman GF/F filters (0.7 μm), finally collected in 60-mL pre-combusted amber vials. Prior acidification of the DOC samples with 0.2 M ortho-phosphoric acid, samples were kept in the refrigerator. Immediately after collection of CDOM samples, water was filtered through pre-combusted (overnight at 450°C) 25-mm Whatman GF/F filters (0.7 μm) to remove the coarser particles, followed by 25-mm Whatman nucleopore filters (0.2 μm) and stored in 30-mL pre-combusted amber vials for on-board analyses. A multiparameter water quality meter (WTW Multi 3500i) was used in 2014 for water quality monitoring.

Laboratory measurements were generally performed within 1–2 months after the collection. DOC concentrations (μM) were measured by High Temperature Combustion Oxidation (TOC-L CPH, Shimadzu). 100-μL injections of every sample were repeated (three to five times), until the coefficient of variation (CV) of the measurements decreased below 2%. Calibration curves were computed using potassium hydrogen phthalate solution (KHP), ranging from 10 to 400 μM. Measurements of DOC δ^{13}C (δ^{13}DOC) were carried out by wet chemical oxidation (WCO) using a HPLC system coupled to a Delta$^+$ XP IRMS through a LC IsoLink interface (Thermo Fisher Scientific, Germany). This is a flow injection method without using column. Linearity of the system was ascertained using varying concentrations (5–40 mg C L^{-1}) of citric acid (δ^{13}C: −18.58 ‰$_{VPDB}$; Fluka, Germany) and pulses of CO_2 reference gas (δ^{13}C: -38.16 ‰$_{VPDB}$) were used for calibration of the LC-IRMS system during every chromatographic run that lasted for 20 min (more details on LC-IRMS and modifications included; refer to Scheibe et al., 2012).

Colored dissolved organic matter absorption spectra were measured on board following the NASA protocol (Mitchell et al., 2003) every nanometer from 250 to 850 nm using a portable single beam UV-VIS Spectrophotometer (Ocean Optics, JAZ-COMBO) and 10 cm quartz cell. Spectral absorption coefficients

TABLE 1 | Details of spatio-temporal sampling performances during 2012–2017.

Year	Season	Estuary	Sampling strategy	DOM parameters measured
2012	Monsoon	H, S	Salinity-wise	DOC
	Post-monsoon	H, S, T	Salinity-wise	DOC, Chl-a, TSM
2013	Pre-monsoon	S, T, M	Salinity-wise	DOC, Chl-a, TSM
	Post-monsoon	H, S, T, M	Salinity-wise	DOC, Chl-a, TSM
2014	Pre-monsoon	H, S	Salinity-wise	DOC, δ^{13}DOC, TSM
	Post-monsoon	H, S	Time series at S	DOC, DON, TSM
			Salinity-wise at H	DOC, DON, TSM
2015	Monsoon	S, T, M	Salinity-wise	DOC, Chl-a, TSM
2016	Pre-monsoon	H, S, T, M	Salinity-wise	DOC, DON, Chl-a, TSM
	Post-monsoon	H, S, T, M	Salinity-wise	DOC, DON, CDOM, Chl-a, TSM
2017	Pre-monsoon	S, T, M	Time series at S	DOC, CDOM, Chl-a, TSM
			Salinity-wise at T, M	DOC, DON, CDOM, Chl-a, TSM
	Monsoon	S, T, M	Salinity-wise	DOC, DON, CDOM, Chl-a, TSM

Here, H, Hooghly; S, Saptamukhi; T, Thakuran; M, Matla.

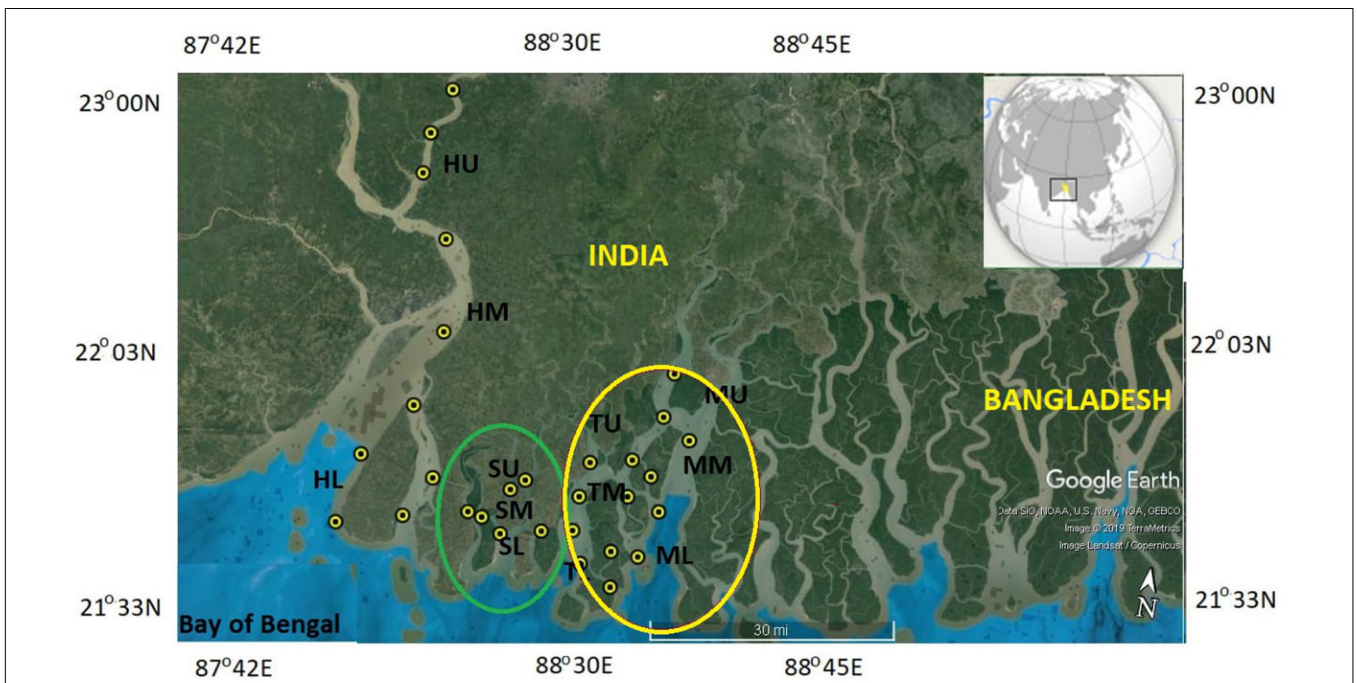

FIGURE 1 | Map of the sampling locations. Latitudes and longitude of many samplings sites overlapped while sampling at the similar points in different surveys (according to geographical positioning system), hence, they were not shown for clarity of the map. Upper (U), mid (M) and low (L) stretches of Hooghly (H), Saptamukhi (S), Thakuran (T), and Matla (M) are presented in the map. Yellow and green circles cover eastern plus central and western part of the Indian Sundarbans, respectively. Map was processed from the Google Earth image.

(m^{-1}) are determined after subtracting the raw absorbance (unitless) measurements with field filtration blanks of UV-oxidized Milli-Q and a null point value an average of absorbance for 695–700 nm. The method of Yamashita and Tanoue (2009) was used to convert absorbance to Napierian absorption coefficient [absorption coefficient $a_{cdom}(\lambda) = 2.303\ A(\lambda)/l$, where A is the measured absorbance at wavelength, λ; l, the cuvette length in meters; and a, the resulting absorption coefficient, m^{-1}]. A wavelength of 350 nm was chosen for consistency with other studies in the coast (Lu et al., 2016). The uncertainty associated with CDOM spectral absorption coefficients at an instrument noise level $<0.005\ m^{-1}$ was on the order of 0.02 to 0.03 m^{-1}. The CDOM spectral slope coefficient (S, nm^{-1}) was determined by fitting a single-exponential non-linear curve to the measured curve from 290–500 nm [$a(\lambda) = a(\lambda_o)e^{-S(\lambda - \lambda o)}$, where $a(\lambda)$ and $a(\lambda_o)$ represent the absorption coefficients at wavelength λ and reference wavelength λ_o] (Shank et al., 2010). The a_{cdom} at 250 nm [a(250)] and 350 nm [a(350)], the spectral slope coefficients between 275 and 295 nm ($S_{275-295}$) and between 350 and 400 nm ($S_{350-400}$), and the slope ratio (S_R) of $S_{275-295}/S_{350-400}$ were

also considered in this study (Helms et al., 2008). Specific UV absorbance (SUVA254; Weishaar et al., 2003) was calculated to provide information on the aromaticity and molecular weight of the bulk DOC pool ($SUVA_{254}$ = $a_{cdom}(\lambda)$/DOC, unit in L mg^{-1} m^{-1}).

Chl-a was extracted under dark condition for approximately 20 h in 10 mL of 90% acetone at 4°C and measured at 630, 645, and 665 nm by UV spectrophotometer (Shimadzu UV 1800) (Strickland and Parsons, 1972). The spectrophotometric method was used for measuring nutrients, mainly dissolved inorganic nitrogen (DIN = nitrite-N + nitrate-N + ammonia-N) and total dissolved nitrogen (TDN). Dissolved organic nitrogen (DON) was calculated by subtracting DIN from TDN and was expressed in μM. (Grasshoff, 1983).

Mixing of Water Masses and DOC

Because of very limited riverine end member input to the Sundarbans estuarine network, in order to quantify the addition or removal of DOC from the estuarine water DOM pool, we applied a simple mixing model, considering mixing of saline creek water and marine BoB water (i.e., water input from BoB). We calculated how theoretically the channel water and the BoB water would mix over a tidal cycle at SM site. Hence, we assumed a box where minimum tidal height or the reference height (H_R) was 0.2 m (low tide at 05:00, March 30, 2017) and maximum height was 3.3 m (high tide at 11:00, March 29, 2017). Based on the changes in water level (i.e., $\Delta H = H_{obs} - H_R$) we calculated the contribution of channel water and BoB water to the total water mass as per then below formulations:

1. Contribution of channel water: $W_{channel}$ (%) = $100 - (100 \times \Delta H/H_{obs})$
2. Contribution of BoB water (%) = $100 - W_{channel}$.

Now, due to the conservative mixing of channel water ($W_{channel}$) and BoB water (W_{BoB}), expected DOC concentrations in each tide were calculated, following mass based equation:

3. $C_{exp} = W_{channel}/100 \times C_{channel} + W_{BoB}/100 \times C_{BoB}$;

where $C_{channel}$ denotes observed DOC in the channel water at each tide, whereas C_{BoB} means DOC concentration from the BoB (C_{BoB} = 88 μM; reported by Shah et al., 2018).

Therefore, the "added" or "subtracted" DOC in the mangrove estuarine system was represented:

4. $C_{add/sub} = C_{obs} - C_{exp}$.

We applied SRTM digital elevation model (ArcMap) to figure out elevation data for the Lothain Island (i.e., SM in **Figure 1**) where a 24-h time series survey was conducted. The assumption that "mangrove" creek water and BoB water mixes conservatively fitted for this study site quite well, because most of the pixels having elevation of 3–5 m (refers to supplementary image of SRTM, **Supplementary Figure S1**) was in line with the average tidal height, confirming very little changes on water volume. Furthermore, elevation data showed that there were hardly any slopes, as most of the pixels had the same elevation. We roughly estimated the slope based on arc (sin) and found it to be very small, suggesting not much important changes on the water volume. Parvathy and Bhaskaran (2017) provided a detailed review showing Sundarbans a low-wave energy coast with gentle bottom slopes and gradual topography. It is therefore reliable to assume symmetrical water column bathymetry at least for the channel at SM site where time series observation was conducted, allowing tidal height as main function of water level changes.

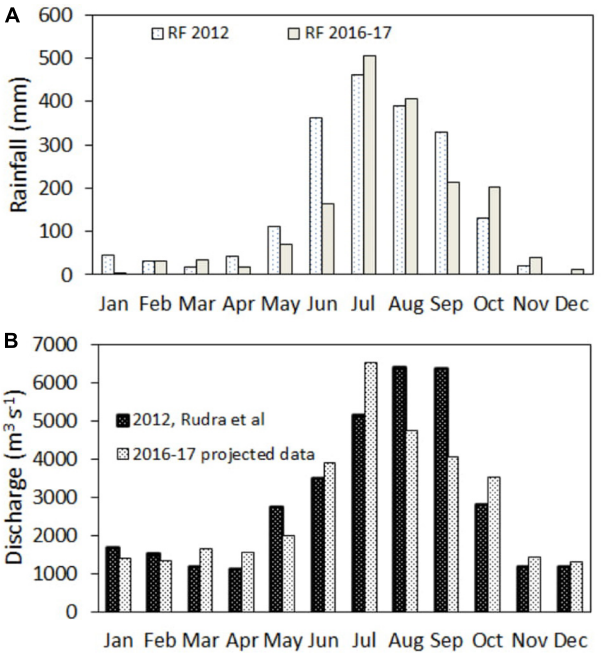

FIGURE 2 | (A) Rainfall (RF, in mm) in 2012 and mean RF of 2016–2017 and, **(B)** observed freshwater discharge (m^3 s^{-1}) of the Hooghly River in 2012 by Rudra (2014) and projected mean discharge in 2016–2017. Meteorological data for 2012, 2016, and 2017 were retrieved from NOAA, ARL database (http://www.arl.noaa.gov/ready.html).

Calculation of DOM Loading

Annual loading of DOC and seasonal loading of CDOM from the Hooghly estuary were calculated from monthly river discharge and respective concentration data. Since we only have direct river discharge records available for 2011–2012 by Rudra (2014), which did not correspond to our observation period, we applied an indirect method to estimate river discharge in 2016–2017. We drew a correlation between rainfall and water discharge data, extrapolated using rainfall observed in 2016–2017, and showed if the difference was statistically significant or not. The linear significant correlation equation between observed rainfall (RF, mm) and river discharge (m^3 s^{-1}) in 2011–2012 (river discharge = 10.73.RF + 1168; r^2 = 0.82; **Supplementary Figure S2**) was used to calculate discharge for 2016 and 2017 (here, RF is a known variable; data taken from http://www.arl.noaa.gov/ready.htm). Averaging monthly rainfall in 2016 and 2017, we calculated projected mean river discharge (**Figure 2A**). Projected and observed discharge data reached

best agreement with RMSE (square root of the mean of the squared prediction error) at the minimum (800 m^3 s^{-1}), and the difference between interannual river discharge data were statistically insignificant (T-stat = 0.40, p = 0.85) because water volume is large and any little difference in rainfall would not give significant difference of water flow, as there is always certain amount of major water discharge from the Farakka barrage upstream of the Hooghly.

Annual loading of DOC and post-monsoonal loading of CDOM were determined from their freshwater end member values as 290 ± 67 and 6.10 ± 1.0 m^{-1}, respectively (averaging data collected from four sampling sites upstream at seasonal scale, salinity = 0.22) and projected freshwater discharge data for 2016–2017 ranging from 1,302 to 6,546 m^3 s^{-1} and averaging 2,786 m^3 s^{-1} (**Figure 2B**). For CDOM loading, only post-monsoonal river discharge (1,368 m^3 s^{-1}) was considered. Loading values were normalized to the estuarine area to allow comparison of yields of riverine estuary and mangrove dominated estuaries. Catchment area of the Hooghly estuary is 60,000 km^2 (refers to Mukhopadhyay et al., 2006).

Groundwater discharge/porewater exchange has been suggested to influence carbon cycling in the mangrove and estuarine environments (Santos et al., 2012; Sadat-Noori et al., 2016). However, groundwater inputs to coastal waters may be volumetrically small when compared to surface water inputs in macro-tidal environment like the Sundarbans. This research also lacked natural groundwater tracers (^{233}Ra and ^{224}Ra) and pore water DOC samples for carrying out such analyses. Hence, accepting this as a limitation of our study, we keep the current flux for the surface water DOM only.

Data Analysis

Statistical analysis was performed using IBM SPSS 20 Statistics (v 1.0.0.0). For the purpose of examining the differences between two groups, we used the paired T-test. A one-way analysis of variance (ANOVA) was employed to test variance between the means of multiple stations. Simple regression (relationships with salinity and between measured DOM parameters, i.e., DOC and absorption properties and water quality parameters such as salinity, DO, TSM, and Chl-a) were applied to define the coefficient of determination (r^2) between variables. A principal component analysis (PCA) was performed to examine DOM evolution during its estuarine transport (XLSTAT, trial version 2019). Bulk DOC, optical properties of CDOM (e.g., $a_{cdom}350$, $S_{275-295}$, slope ratio, $SUVA_{254}$) and related water quality parameters, were used as variables.

RESULTS

Spatio-Temporal Distribution of DOC

This study documented the variations of DOC concentrations and other related physicochemical parameters in the mangrove and riverine waters. A summary of the investigated DOM and water quality parameters for four estuaries are given in **Table 2**. Furthermore, a detailed description of the results (including sampling sites and periods) can be retrieved from the **Supplementary Table S1**.

Mean salinity in the Hooghly estuary and Sundarbans estuaries (i.e., Saptamukhi, Thakuran, and Matla) ranged from 0.5 ± 0.2 to 15 ± 10 and 18 ± 8 to 26 ± 7, respectively. Salinity gradient along the Hooghly estuary was very prominent, unlike the mangrove estuaries, where salinity changes were inconsistent along the estuarine transect. Little change in DO concentration was observed in all four estuaries (ranging 5.6 ± 1.3 mg L^{-1} to 7.5 ± 1.4 mg L^{-1}; n = 135). By contrast, mean surface water Chl-a concentration varied significantly among the estuaries (p = 0.05, F = 3.85, n = 92). The Chl-a and DO concentration increased downstream of the Hooghly, but such trend was not very apparent for the mangrove estuaries. The Matla and Hooghly were relatively turbid than the Saptamukhi and Thakuran as indicated by their higher TSM content (n = 112). In most of the surveys, Secchi disc transparencies were below 1 m.

Overall mean DOC concentrations were higher in the Hooghly estuarine water than the mangrove waters (366–478 vs. 226–283 μM; n = 146). The same pattern was observed for the DON concentrations as well (mean values: Hooghly, 12–132 μM; Sundarbans, 6–70 μM; n = 82). DOC:DON ratio ranged from 1.8 to 139, and higher ratios were calculated for the three mangrove estuaries (averaging 15.5) than the Hooghly river estuary (5.6). The δ^{13}DOC increased from −25.3 to −24.3‰ along the salinity gradient of the Hooghly toward the BoB end (data used from Ray et al., 2015).

Scatter plot of DOC and other water parameters showed their interannual changes along the salinity gradient from 2012 to 2017 (**Figure 3**). Non-conservative trend of DOC was observed all along the estuarine transect. Interannual variations of DOC (p = 0.003), TSM (p = 0.005), and DO (p = 0.02) were statistically significant, unlike Chl-a (p = 0.08). Maximum concentrations of DOC and DO were recorded in 2016 (365 ± 104 and 6.4 ± 0.6 μM, respectively; n = 52) while minimum DOC was measured in 2017 (188 ± 66 μM; n = 38) when TSM was highest (493 ± 266 mg L^{-1}).

Significant differences in water column profiles of salinity, DO, and DOC pattern were observed for all four estuaries (**Figure 4**; DO data not shown). Generally, DOC in the bottom water was found to be 1- to 1.5-times higher than the surface water, while DO showed a reverse trend. Maximum difference between the surface and bottom water DOC was observed for the SM, SL, and MU sites and for the ML site during the post-monsoon. Salinity change along the water column was not always consistent; rather, it depended on station locations and seasons.

During the 24-h time series observation, salinity varied according to tidal height, except at 04:00 when an abrupt rise in salinity was recorded during receding tide (**Figure 5A**). Tidal pattern of DO and Chl-a were not very consistent (**Figures 5B,C**). However, minimum DO was recorded at lowest tide (4.73 mg L^{-1} at 17:00) and maximum at nearly highest tide (6.75 mg L^{-1} at 21:00). No tidal variation was observed in Chl-a concentration that ranged from 1.8 to 4.0 μgL^{-1} (n = 13). Tidal pattern of DOC showed generally decreasing concentration during the

TABLE 2 | Water physicochemical parameters, DOC and optical absorption properties along the longitudinal transects of four estuaries during the sampling period between 2012 and 2017 (mean ± SD).

Estuaries	Salinity	DO mg L^{-1}	Chl-a μg L^{-1}	TSM mg L^{-1}	DOC μM	DON μM	DOC/ DON	$\delta^{13}C$ ‰	a_{cdom} (350) m^{-1}	$S_{275-295}$ nm^{-1}	$S_{350-400}$ nm^{-1}	S_R	$SUVA_{254}$ L mg^{-1} m^{-1}
Hooghly													
Upper	0.5 ± 0.2 (9)	5.9 ± 0.5 (8)	4.5 ± 2 (8)	240 ± 110 (15)	305 ± 94 (15)	31 ± 23 (9)	9.8	−25.3	6.1 ± 1.8 (4)	0.006	0.013	0.48	5.2
Middle	6.5 ± 5 (8)	5.4 ± 0.6 (6)	4.0 ± 2 (6)	181 ± 124 (14)	478 ± 138 (13)	86 ± 44 (5)	5.5	−24.7	4.2 ± 1.5 (3)	0.007	0.014	0.45	2.5
Lower	15 ± 10 (6)	6.5 ± 0.3 (6)	7.0 ± 4 (4)	115 ± 45 (6)	366 ± 87 (7)	95 ± 43 (7)	3.8	−24.3	5.1 ± 1.2 (2)	0.006	0.012	0.48	3.2
Saptamukhi													
Upper	18 ± 8 (10)	5.5 ± 0.7 (10)	5.6 ± 3 (9)	62 ± 30 (8)	259 ± 76 (8)	32 ± 14 (4)	8.0	−24.5	3.4 ± 1.2 (5)	0.004	0.015	0.28	2.5
Middle	21 ± 9 (36)	6.2 ± 0.5 (30)	4.0 ± 2 (17)	76 ± 37 (16)	226 ± 92 (39)	30 ± 11 (32)	7.5	−23.9	4.3 ± 1.1 (4)	0.005	0.014	0.29	2.4
Lower	27 ± 4 (9)	5.4 ± 0.7 (9)	4.4 ± 2 (8)	67 ± 47 (9)	249 ± 80 (8)	13 ± 7 (8)	19	n.d	2.8 ± 0.8 (2)	0.007	0.020	0.35	3.3
Thakuran													
Upper	20 ± 9 (7)	5.7 ± 0.6 (7)	2.3 ± 2 (5)	82 ± 44 (7)	283 ± 103 (5)	26 ± 17 (3)	10.8	n.d	4.0 ± 1.4 (4)	0.003	0.016	0.20	3.8
Middle	25 ± 4 (7)	6.4 ± 0.3 (7)	2.6 ± 1 (6)	91 ± 57 (8)	264 ± 92 (11)	10 ± 8 (2)	26.4	n.d	3.0 ± 0.5 (3)	0.002	0.016	0.16	4.1
Lower	26 ± 9 (6)	6.5 ± 0.4 (6)	2.2 ± 2 (4)	73 ± 41 (9)	248 ± 116 (7)	18 ± 2 (2)	13.7	n.d	2.9 ± 0.3 (2)	0.005	0.021	0.22	5.5
Matla													
Upper	22 ± 8 (8)	6.6 ± 0.8 (8)	3.8 ± 1 (7)	156 ± 146 (7)	286 ± 123 (12)	42 ± 21 (7)	6.8	n.d	3.6 ± 0.9 (4)	0.005	0.017	0.25	4.5
Middle	25 ± 5 (9)	7.9 ± 0.7 (8)	4.7 ± 1 (6)	132 ± 65 (10)	258 ± 107 (9)	22 ± 5 (5)	11.7	n.d	2.8 ± 0.2 (4)	0.003	0.017	0.18	4.3
Lower	26 ± 7 (16)	6.5 ± 0.5 (12)	2.2 ± 2 (4)	135 ± 80 (8)	254 ± 60 (12)	12 ± 2 (4)	21	n.d	3.4 ± 0.5 (4)	0.006	0.018	0.36	4.3

*n = number of samples; these numbers varied among different parameters according to station locations and priorities in analytical measurements. The δ^{13}DOC values were taken from Ray et al. (2015) (full data available as **Supplementary Table S1**). n.d. = no data available.*

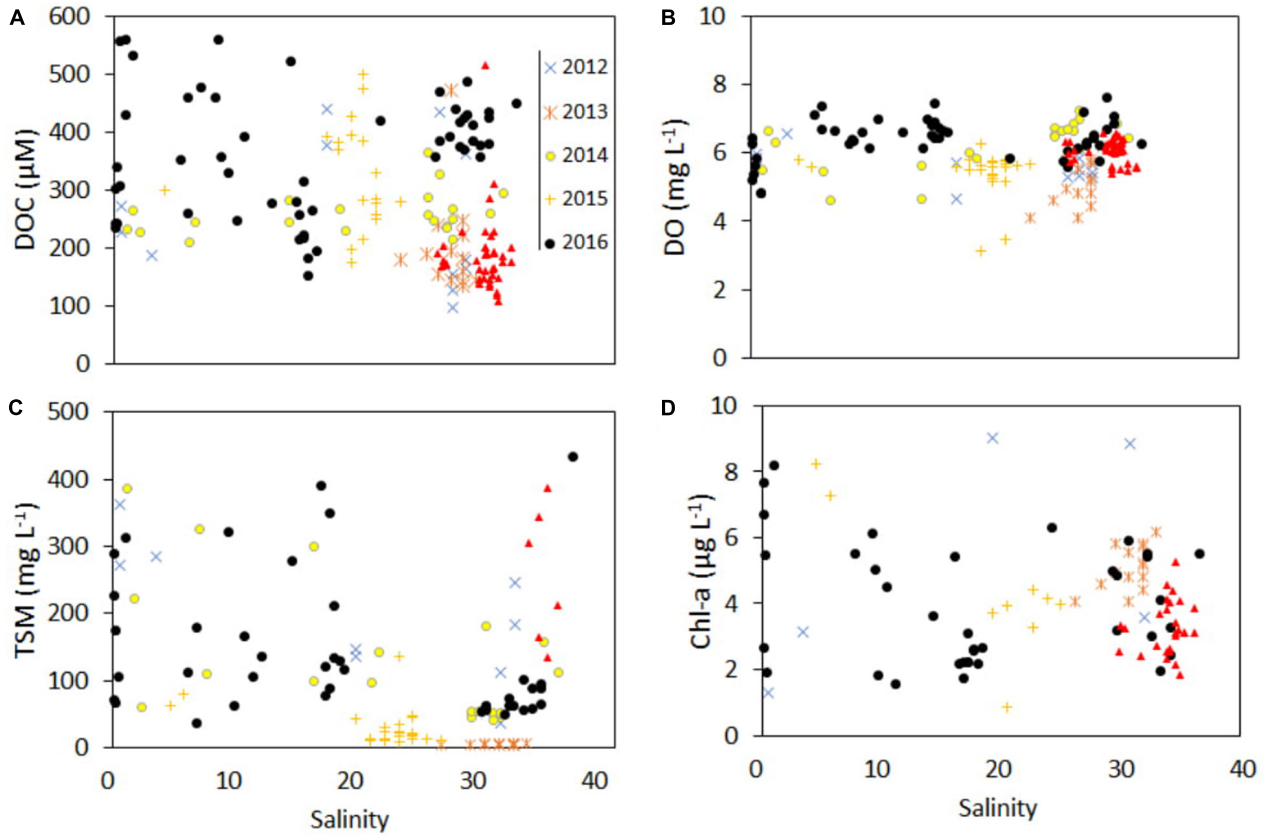

FIGURE 3 | Distribution of **(A)** DOC (μM), **(B)** DO (mg L^{-1}), **(C)** TSM (mg L^{-1}), and **(D)** Chl-a (μg L^{-1}) as a function of salinity and year (2012–2017).

high tide (excepting at 21:00 and 22:00 h) and increasing concentration during the low tide. At an hourly basis, DOC ranged between 109 and 286 μM in a full tidal cycle (n = 24). Observed DOC was always higher than its expected conservative mixing values (ranging 90−172 μM), resulting in all positive "added C" or ΔC (ranging 20−122 μM). The mixing pattern of channel water and BoB water showed clear variation with increasing contribution (%) of channel water (and decreasing BoB water) during the low tide and vice versa for the high tide (**Figure 5D**).

Spatio-Temporal Distribution of CDOM Absorption Properties

Similar to DOC distribution pattern, CDOM absorption coefficient at 350 nm or $a_{cdom}(350)$ was quite higher at the Hooghly estuarine sites (mean ranging 4.2 to 6.1 m^{-1}; n = 9) than at the mangrove estuarine sites (mean ranging 2.8 to 4.3 m^{-1}; n = 32) (**Table 2**). Scattered plot showed negative correlation of $a_{cdom}(350)$ with salinity down the Hooghly estuary (r^2 = 0.45, **Figure 6A**) that was opposite to the trend of mangrove estuaries (r^2 = 0.30), indicating dynamic biogeochemical occurrences within the CDOM distribution pattern (**Figure 6A**). Polynomial fit of slope at 275–295 nm ($S_{275-295}$) showed significant negative deviation toward the lower stretch of the Hooghly (r^2 = 0.66) ranging from 0.004 to 0.006 nm^{-1}, but such a correlation was never observed for the mangrove estuaries, where $S_{275-295}$ widely ranged from 0.001 to 0.009 nm^{-1} (**Figure 6B**). Slope ratio (S_R) at 275–295 nm and 350–400 nm differed among the estuaries and followed similar trend like $S_{275-295}$; however, the values were twofold higher for the Hooghly river estuary than the mangrove estuaries (**Figure 6C**). Calculated high CV (%) in $S_{275-295}$ (61%) and S_R ratios (57%) indicated wide distribution of DOM sources. $SUVA_{254}$ mirrored the changes of $a_{cdom}(350)$ with a negative slope along the Hooghly estuarine gradient (r^2 = 0.46) and a positive slope along the mangrove estuaries (r^2 = 0.71) (**Figure 6D**). Observed mean $SUVA_{254}$ in the Thakuran and Matla estuary were relatively higher than the Saptamukhi estuary. Here we have also calculated the spectral slope coefficients of CDOM at 290–500 nm, that varied along the Hooghly and mangrove dominated estuaries from the river end (salinity = 0.0; $S_{290-500}$ = 0.014 nm^{-1}) to the sea end (salinity = 31; $S_{290-500}$ = 0.022 nm^{-1}). Seasonally for the mangrove dominated estuaries, the highest $a_{cdom}(350)$ and corresponding lowest $S_{290-500\ nm}$ were observed in the monsoon (3.91 ± 0.89 m^{-1} and 0.016 ± 0.002 nm^{-1}, respectively), followed by post-monsoon (2.66 ± 0.17m^{-1} and 0.017 ± 0.002nm^{-1}) and pre-monsoon (3.4 ± 0.62 and 0.019 ± 0.002 nm^{-1}) ($S_{290-500}$ data are not shown).

CDOM optical properties varied slightly according to tide. The $a_{cdom}(350)$ was relatively high at low tide (5.9 ± 2.3

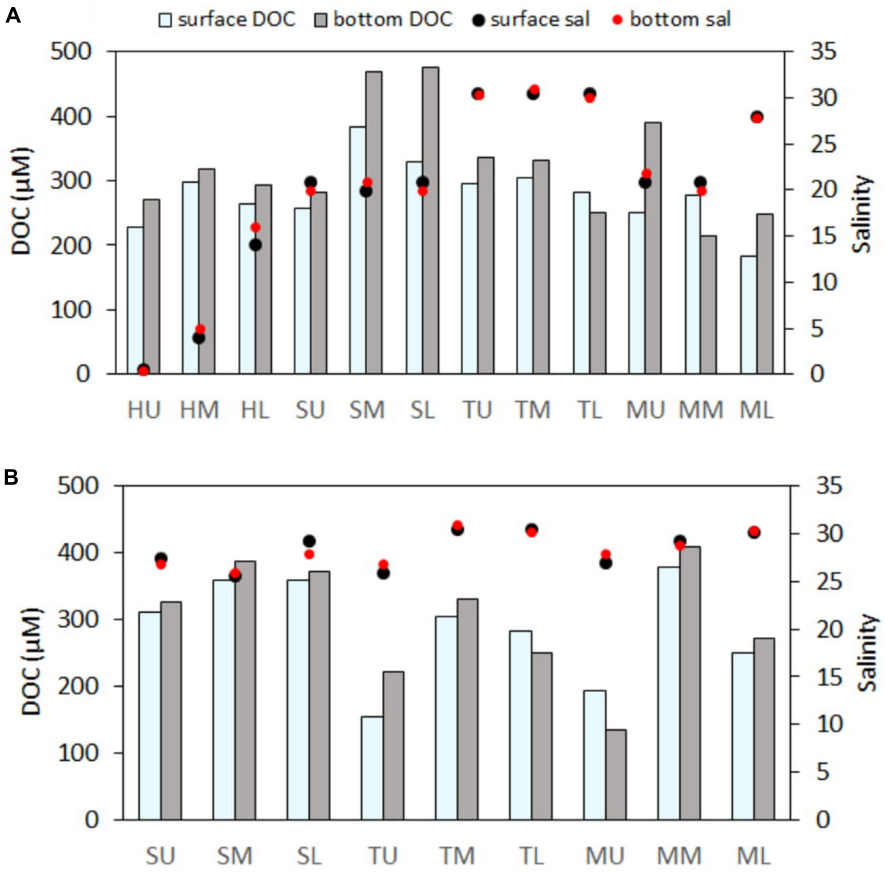

FIGURE 4 | Water column variability of DOC (µM) and salinity in panels **(A)** post-monsoon and **(B)** pre-monsoon.

m^{-1}, 14–18:00 and 02–8:00 h) than high tide (4.9 ± 0.9 m^{-1}, 10–0:00 and 08–12:00 h) (n = 11, **Figure 7A**). Temporal evolution of $S_{275-295}$ was not always consistent, although slightly lower values were achieved during the low tide conditions (0.004), compared to the high tide (0.005) (**Figure 7B**). The slope ratio mirrored the changes of $S_{275-295}$ (**Figure 7C**). $SUVA_{254}$ was nearly comparable in both tides, only little higher at low tide (5.5 ± 1.9 L mg^{-1} m^{-1}) than high tide (5.3 ± 1.7 L mg^{-1} m^{-1}) (**Figure 7D**).

PCA Result

The first two principal components (F1 and F2) accounted for 55.5% of the total variance (39 observations for each variable) (**Figure 8**). Along the first PC (F1), DOC, Chl-a, and all optical properties are distributed as positive loadings at second PC (F2), salinity, TSM and slope properties, $SUVA_{254}$, and Chl-a are dispersed as negative loadings. Maximum loadings were observed for F1 with highest contributions from $a_{cdom}(350)$, slope ratio, and DOC (28%, 27%, and 10%, respectively). Correlations among the variable and factors revealed significant positive relationships between DOC and CDOM. The distribution of sampling stations was highly heterogeneous, as evident from the Strahler order and score plot (figure not shown).

DISCUSSION

Hydrographic Trend and Water Quality

Climatological conditions (air temperature, rainfall, and humidity) along the northeast coast of BoB are largely driven by the annual movement of the Inter-Tropical Convergence Zone (ITCZ). The Hooghly Sundarbans estuarine wetland experienced maximum rainfall during the monsoon periods of 2012, 2016, and 2017 (150–540 mm, **Figure 2A**) when riverine discharge from the Hooghly upstream was at peak (3,496–6,416 m^3 s^{-1}, recorded at HL sites in 2012 by Rudra, 2014, and projected data 3,809–6,546 m^3 s^{-1}, **Figure 2B**). The other two seasons were relatively dry with minimal rainfall and river discharge. Subsequently, water quality parameters like salinity, water temperature, dissolved oxygen, suspended matter, Secchi depth, pigment content, and nutrients would largely alter upon seasonal changes. Significant monsoonal influence on water quality and primary productivity of the Hooghly river and the Sundarbans mangrove estuaries has been amply documented in previous studies (works of Biswas et al., 2004; Mukhopadhyay et al., 2006; Choudhury and Pal, 2010; De et al., 2011; Roshith et al., 2018). In the subsequent discussion, we will discuss temporal evolutions of DOC and optical properties driven by the hydrology, catchment

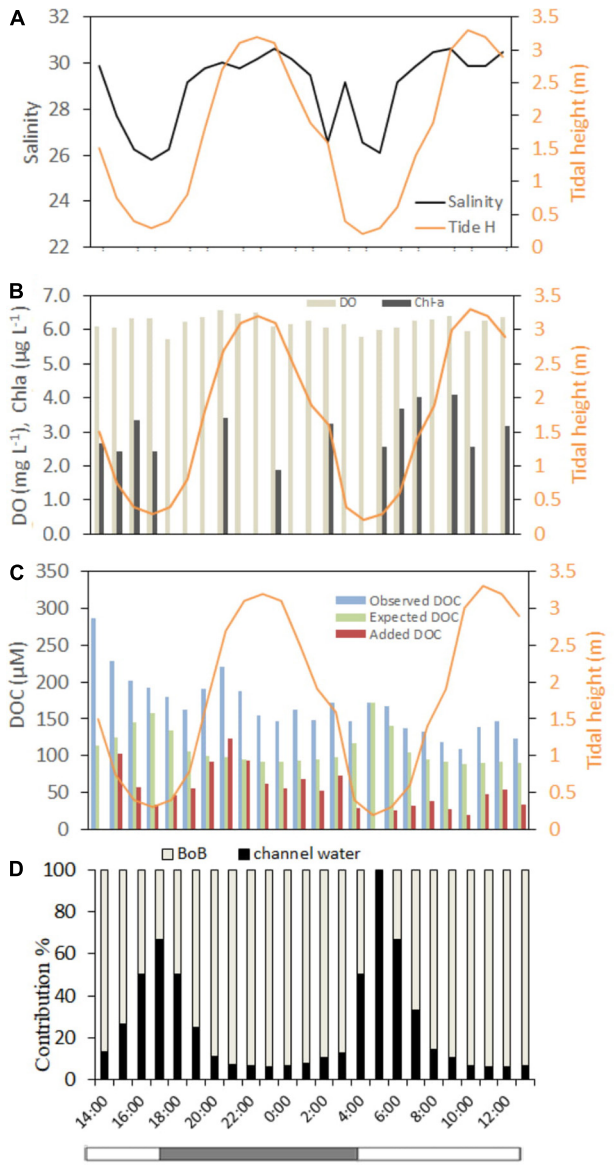

FIGURE 5 | Hourly distribution of **(A)** salinity and tidal height (m), **(B)** DO (mg L^{-1}), Chl-a (µg L^{-1}), and **(C)** DOC (µM) during the 24-hr observation in the Saptamukhi estuary (point SM). **(D)** Tidal contribution (%) of channel water and water from Bay of Bengal (BoB) were shown.

characteristics, and biogeochemical processes occurring within the dynamic estuarine regions of the Sundarbans.

Spatio-Temporal Dynamics of DOC and CDOM

Unlike DOC, CDOM data collected from the Hooghly Sundarbans estuarine system are limited for the present study. Interannual variability of CDOM could not be achieved for either of the systems, whereas for seasonality, only post-monsoonal pattern for Hooghly and complete seasonal data for the Sundarbans were available. Therefore, it is unlikely to predict any discernable changes in CDOM during the observation tenure due to increasing or decreasing DOC level, or other biogeochemical and/or hydrological features, thus creating gaps in identifying the sources and transformation of C along the mixing zones of the estuaries. Accepting this as a limitation of our current research and further recommending covering all essential DOM parameters (i.e., DOC, δ^{13}DOC, and CDOM) during sampling along the Hooghly Sundarbans estuaries, we have progressed our discussions in the subsequent paragraphs.

DOM in the mangrove surrounded estuarine region of the Sundarbans has been suggested to be derived from a diverse array of both allochthonous (litter leaching) and autochthonous (marine algae) sources (2018a). In our previous pre-monsoonal observation, the relationship between δ^{13}C of particulate OM versus $(C:N)_{atomic}$ ratio confirmed similarity of DOM composition of the mangroves with that from Hooghly riverine transport (Ray et al., 2015). However, because our previous study suffered from large-scale spatio-temporal data of DOC, water quality parameters, and CDOM measurement, we anticipated variability in DOM sources and distribution over a wide section of the ecosystem. Therefore, to achieve a more comprehensive understanding on estuarine DOM biogeochemistry, we included our previously published results of DOC and its isotope, collected from the Hooghly and Saptamukhi estuary in 2014 during the pre-monsoon and post-monsoon periods.

Riverine inputs, autochthonous production from algal and vascular plants, benthic fluxes, groundwater inputs, and exchange with adjacent coastal systems are generally said to be the major sources of DOM in estuaries (Bianchi, 2006). Riverine and anthropogenic inputs (i.e., allochthonous origin) from the populated catchments mainly govern OM supply into the Hooghly waters throughout the year. Elevated anthropogenic sources, such as untreated or semi-treated industrial sewage, municipal loads, and phosphate fertilizers, have been previously documented for the in the Hooghly estuarine waters (De et al., 2010; Sarkar et al., 2017). Clearly and consistently, ∼1.5-times-higher DOC could be observed along the Hooghly riverine stretches, compared to the nearest Saptamukhi estuary. The estuarine gradient of DOC was not very prominent for the Hooghly because of non-conservative mixing of the river water and BoB water, although slightly negative concentration gradient could be achieved along the mangrove estuarine transect due to mixing of low concentration marine DOC present in the BoB water. Temporal variability of DOC concentration in the surface water was quite high, because of seasonal effects. DOC concentration for the Hooghly estuary and three other estuaries of the Sundarbans were averaged separately according to monsoon, pre-monsoon, and post-monsoon. DOC differed significantly between monsoon and non-monsoon periods (student's T-test, $T_{stat} = 2.30$; $p = 0.05$), being highest during the post-monsoon in the mangrove estuaries (316 ± 84 µM), whereas monsoonal collections resulted in lowest DOC concentration for the Hooghly estuary (249 ± 31 µM) (**Figure 9**). Reasons for such temporal variations of DOC mainly include seasonal discharge fluctuations, particularly during the peak flow in monsoon (June–September). Reduction of DOC concentration

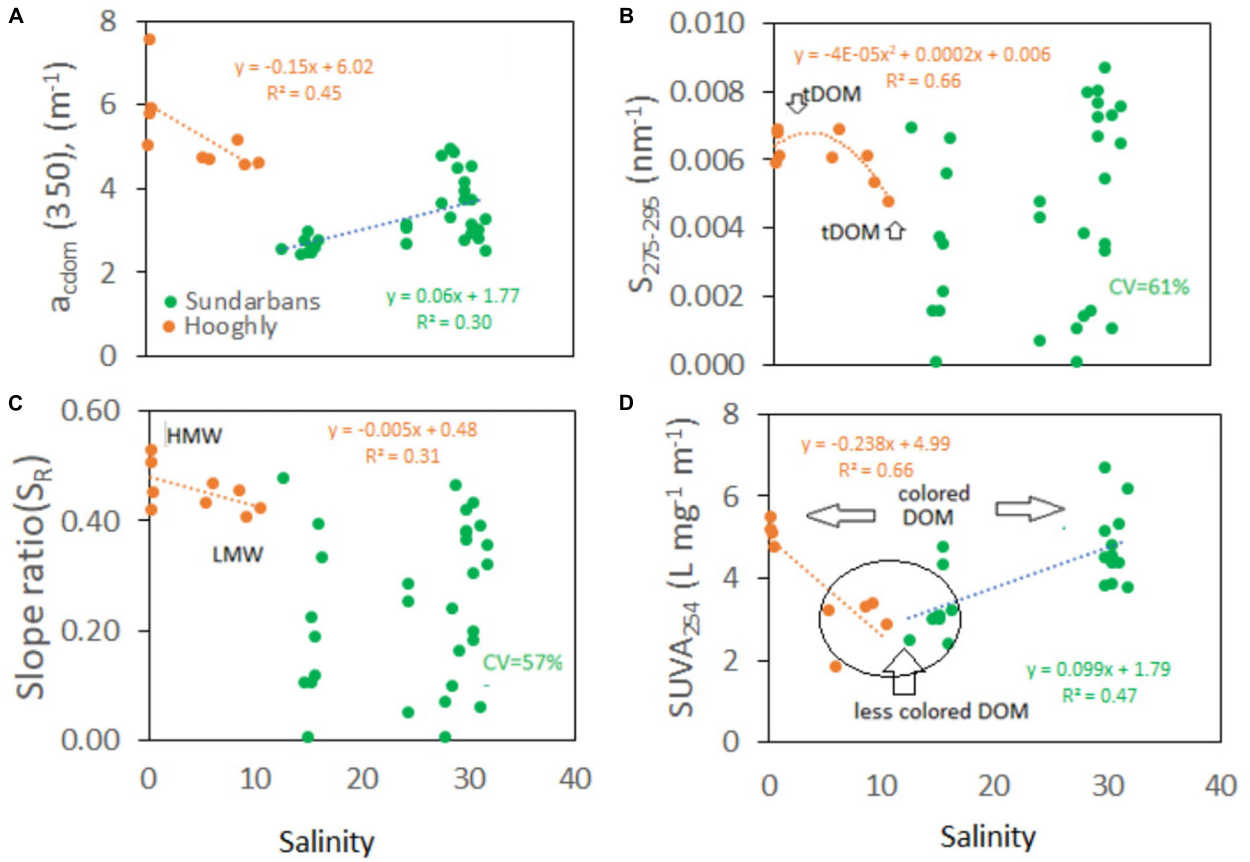

FIGURE 6 | Distribution of **(A)** $a_{cdom}(350)$ m^{-1}, **(B)** slope at 275 and 295 nm, **(C)** slope ratio (SR) between 275–295 and 250–400 nm, and **(D)** $SUVA_{254}$ (L mg^{-1} m^{-1}). CV: coefficient of variance, HMW: high molecular weight, LMW: low molecular weight, tDOM: terrigenous DOM, $SUVA_{254}$: specific UV absorption at 254 nm.

in monsoon could be due to a dilution effect by increased water flux from the Farakka barrage (located 285 km upstream from the mouth of the Hooghly) and rainfall, the latter likely being more important for the Sundarbans estuaries. Changes in DOM due to heavy rainwater was documented for the subtropical Fukido mangroves in Japan by Kida et al. (2019). Shortest water residence time during monsoon (4.7 days, and 18.6–24.5 days for non-monsoonal period for Hooghly estuary; Mukhopadhyay et al., 2006) could explain the faster removal of C from the water column to the BoB. Surface salinity data confirmed strong seasonal and interannual variability of surface water masses during the pre-monsoon and monsoon. On other hand, DOC enrichment during post-monsoon in the mangrove waters could be primarily linked to higher litter leaching, as maximum litter input was recorded at the similar study sites and periods in our previous observations (Ray et al., 2011).

Optical properties of CDOM allow qualitative and quantitative assessment of DOC composition and sources (Vantrepotte et al., 2015). The optical properties of CDOM exhibited considerable spatial variation of spectral slope coefficients, likely due to the presence of Sundarbans mangrove habitat and the extent of exportation and leaching of mangrove detritus. As the CDOM slope values at the river endmember was quite different than the mangrove estuaries, it is reasonable to assume that the mangrove derived CDOM might be characteristically different from its land leaching counterpart. Shank et al. (2010) examined CDOM production from mangrove leaf litter (*Rhizophora* mangle) collected from the Florida Keys, and obtained $S_{290-500}$, ranging between 0.008 and 0.012 nm^{-1}, in line with our observed values (0.016 to 0.019 nm^{-1}). The same authors, under higher laboratory incubation temperatures (32°C), recorded a greater rate of CDOM production (m^{-1} g^{-1} h^{-1}) and corresponding lower slopes ($S_{290-500}$ nm^{-1}) upon senescence stages of leaves, i.e., from orange and yellow (0.35–1.14 and 0.008–0.010, respectively) to brown leaves (0.12–0.15 and 0.014, respectively), suggesting alterations in leaf chemistry in undergoing substantial senescing (Benner et al., 1990; Hernes et al., 2001; Maie et al., 2008). According to our findings, such alterations in mangrove leaf chemistry could be enhanced during the monsoon period (recorded highest $a_{cdom}350$ and lowest $S_{290-500}$; optimum water temperature 29.2 ± 2°C), when major portion of the islands remained inundated, setting ideal conditions for the microbial decomposition of litter components (lignin components), resulting in the loss of structural integrity and promoting

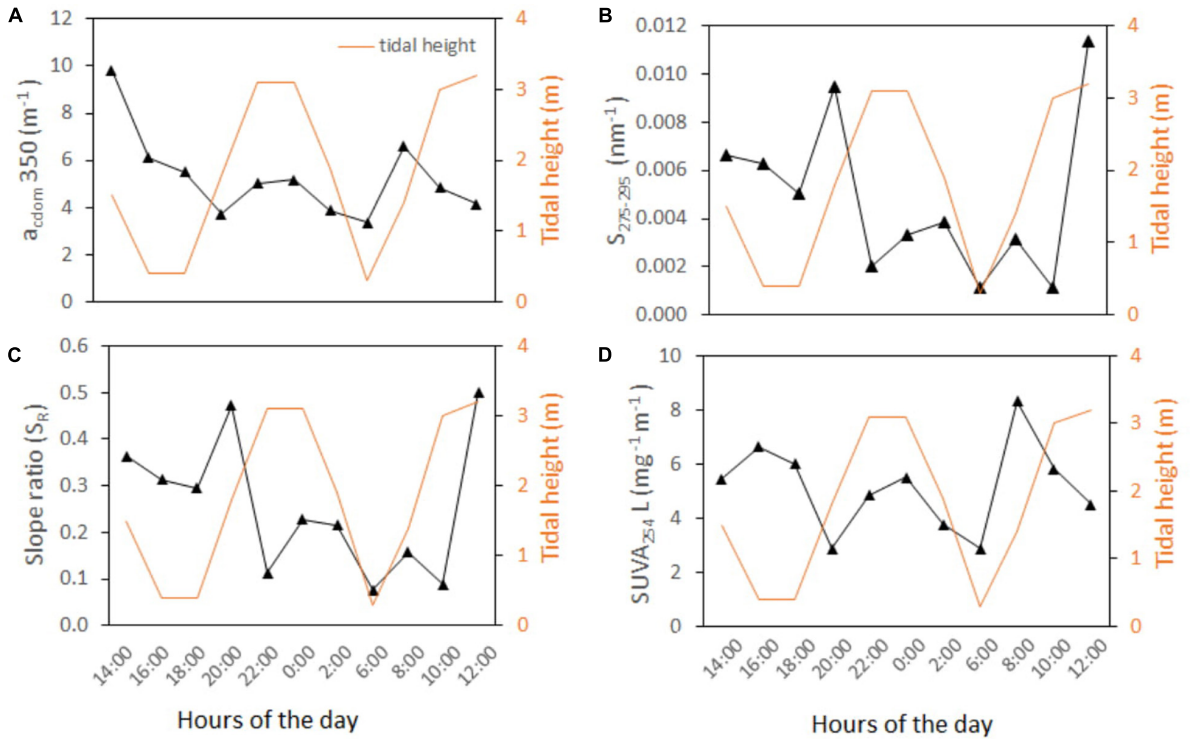

FIGURE 7 | Bi-hourly distribution of **(A)** $a_{cdom}(350)$ m^{-1}, **(B)** slope at 275 and 295 nm, **(C)** slope ratio (SR) between 275–295 and 250–400 nm, and **(D)** $SUVA_{254}$ (L mg^{-1} m^{-1}) during the 24-hr observation in the Saptamukhi estuary (point SM).

leaching of terrigenous CDOM loads (Vähätalo et al., 1998; Forest et al., 2004).

Furthermore, the value of $S_{275-295}$ was used as an index for the contribution of terrigenous DOM (tDOM, Helms et al., 2008) and the degree of photodegradation (Yamashita et al., 2013) in the Hooghly and Sundarbans estuaries. A smaller value of $S_{275-295}$ indicated a greater contribution of tDOM or a lower degree of photodegradation and vice versa (Fichot et al., 2013). Notable variations observed for $a_{cdom}(350)$ over the Hooghly river and the Sundarbans estuaries (2.5 to 7.6 m^{-1}) were within the ranges observed for other tropical estuaries, such as in Taiwan (0.07–12.5 m^{-1}; Yang et al., 2013), the subequatorial mangrove estuary in French Guiana (0.5–4.5 $m^{-1}a_{cdom}$ at 412 nm; Ray et al., 2018b; our result, at 412 nm = 0.8–2.9 m^{-1}), the temperate Ria de Averio estuary in Portugal (4.9–25 m^{-1}; Santos et al., 2016), 30 United States rivers (∼2–12 m^{-1}; Spencer et al., 2012), the Yellow and East China Seas (0.18–0.37 m^{-1}; Zhang et al., 2019), and global ranges for the coastal systems (∼15 m^{-1}; Blough and Del Vecchio, 2002). Such variations resulted from the heterogenous water bodies influenced by anthropogenic input in the optically dense, turbid Hooghly river to the clearer water in the Sundarbans (mean TSM in Hooghly was twice that of Saptamukhi and Thakuran). Slope ratios (0.15–0.53) were slightly lower than the 30 United States rivers (0.7–0.9; Spencer et al., 2012), six major Arctic rivers (0.7–1.1; Stedmon et al., 2011), the Congo river (0.79–1.04; Spencer et al., 2010), and the Taiwan estuary (0.5–4.8; Yang et al., 2013), reflecting enrichment of terrigenous DOM input into the Hooghly Sundarbans system (Helms et al., 2008). Low S could be the result of consistent small values of $S_{275-295}$ derived from CDOM absorption spectra. Mean $S_{275-295}$ is ∼0.005, which is about twofold lower than other mangroves and rivers (see works of Helms et al., 2008; Lu et al., 2016; Ray et al., 2018b). Typically, shallower S indicates DOM with a higher aromatic content and higher molecular weight, which could be obvious in our organic-rich sampling sites influenced by the presence of largest mangrove and drained by the large rivers (like the Ganges). Furthermore, such inconsistency in S might occur from photo-reactivity of CDOM, and such response of S to photodegradation has been attributed to the spectral quality of irradiation (Tzortziou et al., 2007), methodological differences in wavelength ranges used to derive the S parameter in various studies, and also different fitting routines (Spencer et al., 2009). For instance, we observed a shoulder consistently at around 300 nm in the spectrum, which is not very usual for the marine or humic substances, but might be the result of contamination from plastic or phenolics from the mangroves (e.g., tannin leaching from litter). When these methodological differences are accounted for, the response of terrigenous CDOM to irradiation might appear to be consistent. This study had beyond scope to conduct photodegradation experiment or proposing new index in replace of $S_{275-295}$ but could be realized in future.

CDOM absorptions at 440 nm measured by Das et al. (2017) over the continental shore of the northern BoB were lower than

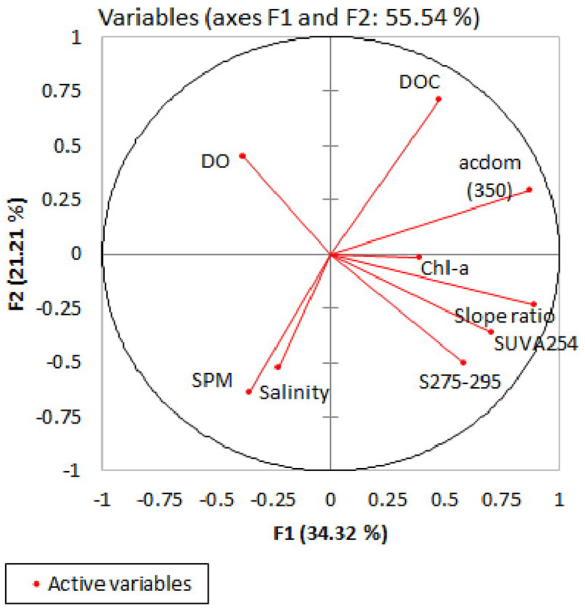

FIGURE 8 | Graphical representation of PCA results for the input variables.

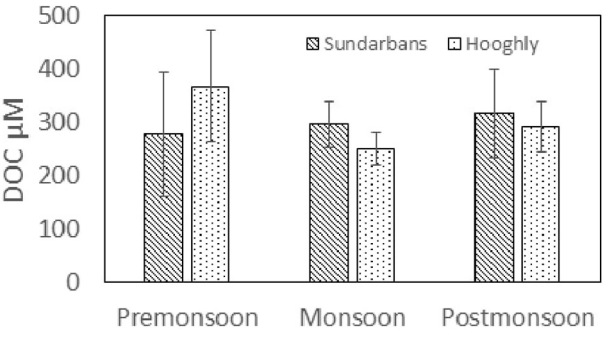

FIGURE 9 | Seasonal variation of mean DOC concentration (µM) for both the Hooghly and Sundarbans estuaries.

our estimates (BoB = 0.1 to 0.6 m^{-1}; this study = 0.4–2.26 m^{-1}, CDOM computed to 440 nm) due to more marine DOM input offshore. A goodness of relationship observed between DOC and CDOM absorptions (DOC = 36.35x + 125.72; r^2 = 0.44; n = 31; **Supplementary Figure S3**) agreed with many other rivers, estuaries, and coastal seas (Blough and Del Vecchio, 2002; Stedmon et al., 2011; Spencer et al., 2012; Yang et al., 2013; Vantrepotte et al., 2015). PCA factor loading also suggested association of DOC with CDOM optical properties (**Figure 8**). The slope of the regression equation (36.35 mol m^{-2}) was within those ranges of 30 United States rivers (23.3–65.1 mol m^{-2}; Spencer et al., 2012) and comparable with other estuarine results (45.5 mol m^{-2} in Taiwan; Yang et al., 2013). We observed positive intercepts between CDOM and DOC for all four estuaries clearly, suggesting that not all DOC is chromophoric. Furthermore, DOC versus CDOM linear regression lines typically become steeper (i.e., increased absorption per unit DOC, in m^{-2} mol^{-1}) in the Matla estuary (0.021), compared to other mangrove estuaries (0.009) and Hooghly (0.001), indicating greater mangrove-derived CDOM input to the eastern part of the Sundarbans. That could be further attested by higher $SUVA_{254}$ (4.4 L mg^{-1} m^{-1}), which is known to be positively correlated to the percentage of aromaticity of DOM pool (Weishaar et al., 2003). More tDOM input in the Matla estuary could be evidenced from other DOM properties, such as low Chl-a content (lesser marine algal source) and lower $S_{275-295}$ (more terrigenous signature) (**Table 3**). The possible reason of greater abundance of CDOM in the Matla estuary might be linked to enhanced production of OC/tree (i.e., above-ground and below-ground biomass or AGB and BGB) that ultimately enriched DOM concentration in the adjacent estuary, due to the contribution of plant-derived humic substances leaching from forest sediment and enhanced litter fall (Cai et al., 2017). Earlier we found greater mangrove production in the eastern part of the Indian Sundarbans (AGB + BGB = 65 ± 10 Mg C ha^{-1}; **Table 3**) drained by the Matla compared to the western and central parts (37 ± 3 Mg C ha^{-1}), dominated by the Saptamukhi and Thakuran estuaries.

Transport and Fate of DOM

Hydrological influence on CDOM dynamics is a common observation for the river estuaries (Battin, 1998; Chen et al., 2004; Osburn et al., 2009; Maie et al., 2012; Santos et al., 2016; Kida et al., 2019). Generally, rivers with higher annual discharge exhibit greater CDOM absorption than those with limited freshwater input (observed for United States rivers by Spencer et al., 2013). This trend also applied to our potential sites where $a_{cdom}(350)$ in Hooghly during post-monsoon was an order of magnitude higher than the seasonal data of Saptamukhi, Thakuran, and Matla. Such high CDOM values, specially from the Hooghly upstream sampling locations, resulted in its greater riverine export, contrast to mangrove-derived export (discussed in the next segment). We would expect even higher CDOM in monsoon from the Hooghly stretches due to more terrestrial run off promoted by high discharge. Furthermore, the magnitude of absorption and river flow dependence of CDOM concentration increased with increased distance from the river mouth, indicating greater delivery of DOM via anthropogenic and river input from the Hooghly upstream. Along the salinity gradient of Hooghly estuary, a general decreasing distribution of $a_{cdom}(350)$ and other optical descriptors of DOM molecularity (e.g., $S_{275-295}$ and $SUVA_{254}$, **Figure 6**) revealed removal of tDOM during the transport to BoB. Multiple processes could account for such DOM removal in estuary, such as endmember mixing (De Souza Sierra et al., 1997), DOM photooxidation in stable water of low turbidity (Vodacek et al.,1997), flocculation/precipitation within oligohaline zone (Burton, 1976) or bacterial utilization of DOM (Thurman, 1985; Ogawa et al., 2001).Various laboratory analysis indicated aggregation of humic acid and high molecular DOM onto POM pool (Sholkovitz, 1976) and that also occur best within salinity range between 2 and 4 (Artemyev and Romankevich, 1988). Such a process seems unlikely to dominate as one type of DOM removal mechanism in the Hooghly estuarine water with strong salinity gradient. Furthermore, weak association of

TABLE 3 | Differences of DOC and optical properties between river and mangrove dominated estuaries (AGB, above−ground biomass; BGB, below−ground biomass; 1 Mg = 10^6 g).

Estuarine environment	DOC μM	δ^{13}DOC ‰	a_{cdom} (350 m^{-1})	$S_{275-295}$ nm^{-1}	Slope ratio	$SUVA_{254}$ L mg^{-1} m^{-1}	TSM mg L^{-1}	Chl-a μg L^{-1}	AGB Mg C ha^{-1}	BGB Mg C ha^{-1}
River-dominated	358 ± 116	−25 ± 0.3	5.3 ± 1.7	0.006	0.46 ± 0.04	3.66 ± 1.35	178 ± 30	5.2 ± 1.3	–	–
Mangrove-dominated										
Eastern	216 ± 41	–	3.3 ± 0.6	0.002	0.26 ± 0.13	4.36 ± 1.09	111 ± 72	3.1 ± 0.9	51 ± 13	14 ± 18
Western + central	222 ± 45	−24 ± 0.5	3.5 ± 1.0	0.003	0.25 ± 0.16	3.38 ± 1.74	68 ± 38	4.6 ± 0.6	29 ± 4	8 ± 1

Results are in mean ± SD.

TSM and CDOM optical properties was evident from the PCA factor loadings. Other possible process is the photodegradation of high molecular weight DOM compounds upon UV exposure. However, in turbid estuary like Hooghly where Secchi disc level was consistently low, below 1 m, photobleaching might be unfavorable which is in line with short water residence time of even less than a week during the monsoon, whereas photo-oxidized decrease in CDOM is observed to be about a month by Vodacek et al. (1997).

Bacterial utilization is an important sink for DOM in estuaries. The Hooghly estuary is putatively heterotrophic in nature, favoring particulate OM decomposition over *in situ* production (Mukhopadhyay et al., 2006; Samanta et al., 2015; Akhand et al., 2016). However, in the case of DOM, it appears that bacterial decomposition may be less significant as a "removal" mechanism. To explain more, we discuss the apparent oxygen utilization (AOU = $O_{2equilibrium} - O_{2measured}$) concept, which is a proxy for DOM decomposition. Various studies have shown a significant negative relationship between DOC and AOU for the oceanic water (Kumar et al., 1990; Doval and Hansell, 2000; Shah et al., 2018). From multiple observations at the sampling sites, oxygen undersaturation was very prominent (75–95%) resulting in positive AOU values (35.25−37.20 μM), but contrary to expectations, showing significant positive correlation with DOC (AOU = 0.009 × DOC + 33.7; r^2 = 0.45). Even limited data from the water column suggested no meaningful relationship between DOC increment and DO decrease at the bottom (even few points showed DO increase at depth). While estimating DOC:AOU molar ratio to be −0.13 for the oceanic water of the BoB, Shah et al. (2018) concluded 18% AOU utilization for DOC decomposition. However, such biological remineralization of labile or semi-labile DOM may not hold the same for the upper coastal waters of BoB where our sampling sites are present. In fact, nutrient limitation in those sites could resist bacterial degradation of DOM, but mangrove surrounded estuarine waters are quite nutrient rich as evident from several past works (DIN = 10−20 μM, DIP = 0.5–1.0 μM; Mukhopadhyay et al., 2006; De et al., 2011; Ray et al., 2014; Nandi et al., 2018). Hence, bacterial consumption of estuarine DOM was limited by the refractory nature of DOM, rather than nutrient limitation of the bacterial communities. Another perspective of such positive relationship (DOC × AOU) might be the occurrence of wastewater discharge and anthropogenic stress that might increase both DOC and AOU, particularly in the Hooghly estuary where maximum DOC concentration coincided with maximum AOU. When more DOC enters into the streams via sewage, more ions associated with it are carried and more O_2 is consumed (i.e., AOU increased) to decompose this extra input of OM.

Hence, the deviation from conservative mixing of CDOM along the Hooghly estuary might be connected to mild stratified layers observed within the water column profile of the Hooghly estuary and the mangrove estuaries in the pre- and post-monsoon periods (**Figure 4**). The stratified layer in the Hooghly water column was also traced by Mukhopadhyay et al. (2006), but that was during the monsoon. The consistent evolution of bottom water DOC (averaging 30 μM higher than surface) across the

sampling stations has verified the existence of two DOM pools that have had a distinct composition and optical properties compared to other water mass sources. It is possible that there might exist an old water mass, relative to river water inflow and DOM removal along the estuarine transect, that might be the result of mixing and biogeochemical alteration of sources of the DOM pool. Applying oxygen isotopes in river water, sea water, and groundwater along the Hooghly transect, Samanta et al. (2018) identified an existence of a recirculated seawater component of the submarine groundwater discharge (SGD) to the Hooghly river estuary. That being said, we observed more terrigenous high molecular weight DOM compounds (evidenced by low $S_{275-295}$ and S_R) in the lower stretch of Hooghly to be replaced by less terrigenous low-molecular weight DOM at the freshwater end member where, contrary to the trend, less colored content DOM could be identified (higher $SUVA_{254}$). The tDOM along the mouth of the estuary might be derived from vascular plants like mangroves at Chemaguri (a station near the river mouth), soil leaching, and SGD, and upon extensive mixing with BoB water, it losses a fraction of colored content before exporting to the BoB, in line with the lowering of CDOM absorption over BoB offshore (Das et al., 2017). However, at present, we cannot define the range of this water mass, nor track exactly where it is coming from based solely on available data. All these need to be further investigated by applying radiocarbon dating of DOC specific to water masses along the depth and from distinct freshwater to marine endmember.

Unlike Hooghly, the salinity-versus-CDOM scatter plot for the Sundarbans estuaries showed a positive regression trend; but, we suggest that deviation to be produced from temporal variability, rather than mixing, meaning water salinity in post-monsoon was consistently lower (between 12–16) than other sampling periods (salinity ranging 27–30). Highly non-conservative mixing of CDOM observed in the polyhaline zone of the Saptamukhi, Thakuran, and Matla largely reflected addition of DOM than its removal from the estuarine water. As clearly indicated by the CDOM optical descriptors, prevalence of high molecular weight colored tDOM, most likely being derived from mangrove litter leaching, would enrich DOM pool. However, other sources, such as DOM release via phytoplankton exudation or cell lysis, could also contribute to the CDOM pool (i.e., autochthonous origin). Phytoplankton were reported to contribute 20–26% to the DOC pool (Ray and Shahraki, 2016), while river input was suggested to contribute at large (Ray et al., 2015), but those would be vital sources for the Saptamukhi estuary; but for the Thakuran and Matla, DOM input would most likely be driven by the mangrove vegetation.

DOM Input to the Mangrove Estuary

Statistically significant positive correlation was observed between DOC and CDOM during the 24-h time series observation ($DOC = 17.16 \times a_{cdom}350 + 81.84$; $r^2 = 0.45$). During ebbing tide, surface water DOC and CDOM level increased proportionally with channel water contributions (15 to 70%), probably as a result of enhanced litter leaching via tidal pumping. Few high-DOC values observed at the onset of high tide (such as 187–220 μM against 2.7–3.2 m tidal height) might be indicative of the remainders of high DOC leached from mangroves during ebbing period. Optical analyses revealed that in addition to be a source of DOC for the estuary, mangroves are also very important source of CDOM compounds. Higher $SUVA_{254}$, and simultaneous lower slope ratio and $S_{275-295}$, documented greater delivery of high molecular weight CDOM input to the mangrove estuary. We tested few additional samples of porewater CDOM retrieved from pristine islands in Saptamukhi estuary and manifold higher values of porewater $a_{cdom}(350)$ than the tidal water (at SM: 18.5–26.5 m^{-1}; at SL: 12.7–25.7 m^{-1}; n = 5, our unpublished data) confirmed the benthic pool as one of the major contributors to the estuarine CDOM. In line with this, Ray et al. (2015) described litter leaching and pore water seepage as major pathways of DOM input to the Sundarbans. DON was the major constituent of N in mangrove estuary (∼70% of the TDN) with ∼10- to 15-times higher concentration than the particulate N (2.8–4 μM), implying litter leaching as most significant N loss in mangroves.

Nevertheless, such a general trend of tidally driven DOC input matches with most of other mangrove estuaries as well (Florida, Twilley, 1985; Brazil, Dittmar et al., 2001; Bouillon et al., 2007; de Rezende et al., 2007; and Australia, Maher et al., 2013). End member mixing model between channel water and BoB water produced all positive values of "added DOC" (ΔC) suggesting the Sundarbans estuary to act as a source of DOC. Interestingly, ΔC were even higher when water level was around 2 m (i.e., onset of high tide) and channel water contribution was <15%, that was not very ideal period for mangrove outwelling. Such ambiguity might be attributed to allochthonous input as evidenced by the sudden fall of S_{275-95} and S_R between 20:00 to 22:00 (**Figure 7**). Because a large fraction of DOC is optically active, observed mangrove tidal discharges would have a large influence, not only on estuarine C cycling, but also on the optical properties and CDOM dynamics in the estuary. In addition, mangrove spatial heterogeneity, which has been noticed from varying degree of elevation levels among sites (SRTM image, **Supplementary Figure S1**), should be carefully considered for estimating better resolution DOM fluxes. In doing so, we recommend carrying out time series observations and data collections at multiple locations around the Indian Sundarbans.

Annual DOM Loading From Estuary to Sea

We calculated annual discharge of DOC (10^{11} g C yr^{-1}) and post-monsoonal CDOM (10^{10} m^2 post-monsoon^{-1}) from the Hooghly river to the BoB to be 3.05 ± 0.11 and 8.65 ± 1.42, respectively and area weighted loading or yield to be 5.09 ± 1.17 g C m^{-2} yr^{-1} and 1.41 ± 0.23.$a_{cdom}(350)$ post-monsoon^{-1}, respectively (**Table 4**). As the results of CDOM loading are restricted to post-monsoonal period only, annual extrapolation might be problematic, especially given

TABLE 4 | Annual yield and export of CDOM and DOC from the studied river and mangroves.

DOM production and export	Hooghly River	Sundarbans mangrove
CDOM yield, $a_{cdom}(350)$ month^{-1}	1.41 ± 0.23*	1.77 ± 1.22
CDOM export, 10^{10} m^2 month^{-1}	8.65 ± 1.42*	0.75 ± 0.52
DOC yield, g C m^{-2} year^{-1}	5.09 ± 1.17 (2.38–11.97)	710**
DOC export, 10^{11}g C year^{-1}	3.05 ± 0.11 (1.42–7.18)	30.3**

*Results are in mean ± SD (ranges, where applicable). *For Hooghly, CDOM values are given per post-monsoon (i.e., sum of 4 months); **refers to data from Ray et al. (2018a).*

the high river discharge during the monsoon. However, we still compared at a monthly basis, dividing the results by 4 in post-monsoon, and determined CDOM discharge to be 2.16×10^{10} m^2 month^{-1},and yield as $0.35a_{cdom}(350)$ month^{-1}. From web search, there is no available literature data of CDOM discharge from tropical rivers/estuaries; however, our estimates compared well with those reported for the 15 US rivers (discharge ranging 0.04–30 $\times$ 10^{10} m^2 month^{-1}; mean yield, 0.42 $a_{cdom}(350)$ month^{-1}; Spencer et al., 2013), boreal rivers (discharge 0.02–0.35 $\times$ 10^{10} m^2 month^{-1}, yield ranging 0.13–0.95 $a_{cdom}(375)$ month^{-1}; Asmala et al., 2012), but two- to four-times as high as the highest values of Arctic and Danish rivers presented by Stedmon et al. (2011).

Previously we applied isotope mixing model and quantified mangroves contribution to the total estuarine DOC pool to be 170 ± 42 μM (Ray et al., 2018a). Further using a statistically robust linear relationship between DOC and $a_{cdom}(350)$ observed from the 24-h survey (refers to previous subsection), we calculated mangrove-derived $a_{cdom}(350)$ to be 5.18 ± 3.46 m^{-1}. Multiplying this CDOM value with the net amount of water exchanged between the Sundarbans and BoB in one tidal cycle (i.e., 48×10^9 L day^{-1} from Ray et al., 2018a), we estimated monthly mangrove-derived CDOM discharge to be 0.75 ± 0.52 ($\times$ 10^{10}) m^2 month^{-1} and CDOM yield as 1.77 ± $1.22a_{cdom}(350)$ month^{-1} (**Table 4**). The difference between the CDOM export from the riverine and mangrove estuary to the BoB might be attributed to the higher mean CDOM absorption from the Hooghly upstream compared to the mangrove estuaries [refer to mean $a_{cdom}(350)$ in **Table 2**]. Such difference might be even large during the monsoon, when river discharge is maximally favoring more export of the optically active DOMs via terrestrial run-off. Brandão et al. (2018) showed small input of allochthonous OM (applies to riverine transect here) could have large effect on the spectral line absorption, compared to the large production of autochthonous production of OM (applies to the Sundarbans waters).

In brief, despite monthly riverine CDOM discharge exceeding mangrove-derived estuarine export to the BoB by a factor of 2.8, CDOM yield is greater in the mangrove estuaries than the riverine estuary, which is in line with higher DOC outwelling rate reported for these mangroves (710 g C m^{-2} yr^{-1}, Ray et al., 2018a) compare to its riverine export, higher water exchanged between Sundarbans estuaries and BoB than between the Hooghly and BoB, and also high mangrove productivity delivering more terrigenous type DOM into the creek or estuarine waters.

CONCLUSION

As a recap, both catchment characteristics (mangrove coverage, river input) and estuarine biogeochemical processes contributed to the variations of DOC and CDOM concentrations and compositions in the estuarine environments. Mangrove-derived OM input and forest productivity were among the key controls governing DOM distributions in the Indian Sundarbans, while these were mainly governed by estuarine mixing, fluvial discharge, and anthropogenic stresses from the Hooghly upstream. Optical measurements identified spatially and temporally variant DOM composition covering an extensive sampling stations and periods along the Hooghly river estuary and mangrove dominated estuaries in the Indian Sundarbans. Colored content ($SUVA_{254}$) in DOM pool was higher in mangrove waters than the river waters due to more terrigenous matter input from the former. These optical characteristics are indicative of complex organic compounds such as high-molecular-weight, aromatic-rich DOM. Flux estimates showed greater yield and export of mangrove-derived DOC, but lower export of CDOM to the BoB, as compared to their riverine transport.

DATA AVAILABILITY STATEMENT

All datasets generated for this study are included in the article/**Supplementary Material**.

AUTHOR CONTRIBUTIONS

PS and RR conceived the study with the help of TJ and SM and collected and analyzed the samples along with MP, VG, AA, and SB. SM led the research conducted in the Hooghly Sundarbans. PS together with RR and SM analyzed the data and prepared the manuscript with the guidance of TJ. All co authors reviewed the draft, contributed, and agreed their authorships.

ACKNOWLEDGMENTS

We are thankful to the Ministry of Earth Science, Govt. of India-sponsored Sustained Indian Ocean Biogeochemistry and Ecological Research (SIBER) program (MoES/36/OOIS/SIBER/07) for providing financial support to carry out the study. We thank the Sundarban Biosphere

Reserve (SBR) and Divisional Forest Office (DFO), South 24 Paraganas, Govt. of West Bengal for extending necessary help and support for conducting field work related to this study. We are also thankful to the reviewers for constructive comments and suggestions toward improving the manuscript.

SUPPLEMENTARY MATERIAL

The Supplementary Material for this article can be found online at: https://www.frontiersin.org/articles/10.3389/feart.2020.00218/full#supplementary-material

REFERENCES

Akhand, A., Chanda, A., Manna, S., Das, S., Hazra, S., Roy, R., et al. (2016). A comparison of CO2 dynamics and airwater fluxes in a river dominated estuary and a mangrove dominated marine estuary. *Geophys. Res. Lett.* 43, 11726–11735. doi: 10.1002/2016GL070716

Alongi, D. M. (2014). Carbon cycling and storage in mangrove forests. *Annu. Rev. Mar. Sci.* 6, 195–219. doi: 10.1146/annurev-marine-010213-135020

Arrigo, K. R., and Brown, C. W. (1996). Impact of chromophoric dissolved organic matter on UV inhibition of primary productivity in the sea. *Mar Ecol Prog Ser.* 140, 207–216. doi: 10.3354/meps140207

Artemyev, V. E., and Romankevich, E. A. (1988). "Seasonal variations in the transport of organic matter in North Dvina estuary," in *Transport of Carbon and Minerals in Major World Rivers*, eds E. T. Degens, S. Kempe, and A. S. Naidu (Hamburg: Mitt. Geol.-Palaont. Inst. Univ.), 177–184.

Asmala, E., Stedmon, C. A., and Thomas, D. N. (2012). Linking CDOM spectral absorption to dissolved organic carbon concentrations and loadings in boreal estuaries. *Estuar. Coast Shelf Sci.* 111, 107–117. doi: 10.1016/j.ecss.2012.06.015

Barrón, C., and Duarte, C. M. (2015). Dissolved organic carbon pools and export from the coastal ocean. *Limnol Oceanogr.* 29, 1725–1738. doi: 10.1002/2014gb005056

Battin, T. J. (1998). Dissolved organic matter and its optical properties in a blackwater tributary of the upper Oricono river, Venezuela. *Org. Geochem.* 28, 561–569. doi: 10.1016/s0146-6380(98)00028-x

Bauer, J. E., and Bianchi, T. S. (2011). "Dissolved organic carbon cycling and transformation," in *Treatise on Estuarine and Coastal Science, Vol. 5*, eds E. Wolanski and D. S. McLusky, 7–67.

Benner, R., Weliky, K., and Hedges, J. I. (1990). Early diagenesis of mangrove leaves in a tropical estuary: molecular-level analyses of neutral sugars and lignin-derived phenols. *Geochim. Cosmochim. Acta* 54, 1991–2001. doi: 10.1016/0016-7037(90)90267-o

Bergamaschi, B. A., Krabbenhoft, D. P., Aiken, G. R., Patino, E., Rumbold, D. G., and Orem, W. H. (2012). Tidally driven export of dissolved organic carbon, total mercury, and methyl mercury from a mangrove-dominated estuary. *Environ. Sci. Technol.* 46, 1371–1378. doi: 10.1021/es2029137

Bianchi, T. S. (2006). *Biogeochemistry of Estuaries*. Oxford: Oxford University Press.

Biswas, H., Dey, M., Ganguly, D., De, T. K., Ghosh, S., and Jana, T. K. (2010). Comparative analysis of phytoplankton composition and abundance over a two-decade period at the land ocean boundary of a tropical mangrove ecosystem. *Estuar. Coasts* 33, 384–394. doi: 10.1007/s12237-009-9193-5

Biswas, H., Mukhopadhyay, S. K., De, T. K., Sen, S., and Jana, T. K. (2004). Biogenic controls on the air–water carbon dioxide exchange in the Sundarban mangrove environment, of Bay of Bengal, India. *Limnol. Oceanogr.* 491, 95–101. doi: 10.4319/lo.2004.49.1.0095

Blough, N. V., and Del Vecchio, R. (2002). "Chromophoric DOM in the coastal environment," in *Biogeochemistry of Marine Dissolved Organic Matter*, eds D. Hansell and C. A. Carlson (San Diego, CA: Academic Press), 509–546. doi: 10.1016/b978-012323841-2/50012-9

Bouillon, S., Middelburg, J. J., Dehairs, F., Borges, A. V., Abril, G., Flindt, M. R., et al. (2007). Importance of intertidal sediment processes and pore water exchange on the water column biogeochemistry in a pristine mangrove creek (RasDege, Tanzania). *Biogeoscience* 4, 311–322. doi: 10.5194/bg-4-311-2007

Brandão, L. P. M., Brighenti, L. S., Staehr, P. A., Asmala, E., Massicotte, P., Tonetta, D., et al. (2018). Distinctive effects of allochthonous and autochthonous organic matter on CDOM spectra in a tropical lake. *Biogeosciences* 15, 2931–2943. doi: 10.5194/bg-15-2931-2018

Burton, J. D. (1976). "Basic properties and processes in estuary chemistry," in *Estuarine Chemistry*, eds J. D. Burton and P. S. Liss (London: Academic Press), 1–36.

Cai, D., Xiuhong, Y., Shizhong, W., Yuanqing, C., Jean-Louis, M., Qiu, R., et al. (2017). Effects of dissolved organic matter derived from forest leaf litter on biodegradation of phenanthrene in aqueous phase. *J. Hazard. Mater.* 324, 516–525. doi: 10.1016/j.jhazmat.2016.11.020

Cawley, K. M., Yamashita, Y., Maie, N., and Jaffé, R. (2013). Using optical properties to quantify fringe mangrove inputs to the dissolved organic matter (DOM) pool in a subtropical Estuary. *Estuar. Coast.* 37, 399–410. doi: 10.1007/s12237-013-9681-5

Chari, N. V. H. K., Pandi, S. R., Kanuri, V. V., and Basuri, C. K. (2019). Structural variation of coloured dissolved organic matter during summer and winter seasons in a tropical estuary: a case study. *Mar. Pollut. Bull.* 149:110563. doi: 10.1016/j.marpolbul.2019.110563

Chatterjee, M., Shankar, D., Sen, G. K., Sanyal, P., Sundar, D., and Michael, G. S. (2013). Tidal variations in the Sundarbans Estuarine System, India. *J. Earth Syst. Sci.* 122, 899–933. doi: 10.1007/s12040-013-0314-y

Chen, Z., Lia, Y., and Pan, J. (2004). Distributions of colored dissolved organic matter and dissolved organic carbon in the Pearl River Estuary, China. *Cont. Shelf Res.* 24, 1845–1856. doi: 10.1016/j.csr.2004.06.011

Choudhury, A. K., and Pal, R. (2010). Phytoplankton and nutrient dynamics of shallow coastal stations at Bay of Bengal, Eastern Indian coast. *Aquat. Ecol.* 44, 55–71. doi: 10.1007/s10452-009-9252-9

Coble, P. G. (2007). Marine optical biogeochemistry e the chemistry of ocean color. *Chem. Rev.* 107, 402–418. doi: 10.1021/cr050350%2B

Das, S., Das, I., Giri, S., Chanda, A., and Maity, S. (2017). Chromophoric dissolved organic matter (CDOM) variability over the continental shelf of the northern Bay of Bengal. *Oceanologia* 59, 271–282. doi: 10.1016/j.oceano.2017.03.002

De, T. K., De, M., Das, S., Chowdhury, C., Ray, R., and Jana, T. K. (2011). Phytoplankton abundance in relation to cultural eutrophication at the land ocean boundary of sunderbans, NE Coast of Bay of Bengal, India. *J. Environ. Stud. Sci.* 1, 169–180. doi: 10.1007/s13412-011-0022-3

De, T. K., De, M., Das, S., Ray, R., and Ghosh, P. B. (2010). Level of heavy metals in some edible marine fishes of mangrove dominated tropical estuarine areas of Hooghly River, north east coast of Bay of Bengal, India. *Bull. Environ. Cont. Toxicol.* 85, 385–390. doi: 10.1007/s00128-010-0102-1

de Rezende, C. E., Lacerda, L. D., Ovalle, A. R. C., and Silva, L. F. F. (2007). Dial organic carbon fluctuations in a mangrove tidal creek in Sepetiba bay, Southeast Brazil. *Braz. J. Biol.* 67, 673–680. doi: 10.1590/s1519-69842007000400012

De Souza Sierra, M. M., Donard, O. F. X., and Lamotte, M. (1997). Spectral identification and behavior of dissolve organic fluorescence material during estuarine mixing processes. *Mar. Chem.* 58, 51–58. doi: 10.1016/s0304-4203(97)00025-x

Dittmar, T., Hertkorn, N., Kattner, G., and Lara, R. J. (2006). Mangroves, a major source of dissolved organic carbon to the oceans. *Glob. Biogeochem. Cycles* 20:GB1012. doi: 10.1029/2005GB002570

Dittmar, T., Lara, R. J., and Kattner, G. (2001). River or mangrove? Tracing major organic matter sources in tropical Brazilian coastal waters. *Mar. Chem.* 73, 253–271. doi: 10.1016/s0304-4203(00)00110-9

Doval, M. D., and Hansell, D. A. (2000). Organic carbon and apparent oxygen utilization in the western South Pacific and the central Indian Oceans. *Mar Chem.* 68, 249–264. doi: 10.1016/s0304-4203(99)00081-x

Dutta, M. K., Kumar, S., Mukherjee, R., Sanyal, P., and Mukhopadhyay, S. K. (2019). The post-monsoon carbon biogeochemistry of the Hooghly–Sundarbans estuarine system under different levels of anthropogenic impacts. *Biogeoscience* 16, 289–307. doi: 10.5194/bg-16-289-2019

Fichot, C. G., and Benner, R. (2011). A novel method to estimate DOC concentrations from CDOM absorption coefficients in coastal waters. *Geophys. Res. Lett.* 38:L03610. doi: 10.1029/2010gl046152

Fichot, C. G., Benner, R., Kaiser, K., Shen, Y., Amon, R. M. W., Ogawa, H., et al. (2016). Predicting dissolved lignin phenol concentrations in the coastal ocean

from chromophoric dissolved organic matter (CDOM) absorption coefficients. *Front. Mar. Sci.* 3:7. doi: 10.3389/fmars.2016.00007

Fichot, C. G., Kaiser, K., Hooker, S. B., Amon, R. M., Babin, M., Bélanger, S., et al. (2013). Pan-Arctic distributions of continental runoff in the Arctic Ocean. *Sci. Rep.* 3:1053.

Forest, K., Wan, P., and Preston, C. M. (2004). Catechin and hydroxybenzhydrols as models for the environmental photochemistry of tannins and lignins. *Photochem. Photobiol. Sci.* 3, 463–472.

Fuentes, J. D., Lerdau, M., and Atkinson, R. (2000). Biogenic hydrocarbons in the atmospheric boundary layer: a review. *Bull. Am. Meteorol. Soc.* 81, 1537–1575. doi: 10.1175/1520-0477(2000)081<1537:bhitab>2.3.co;2

Ganju, N. K., Miselis, J. L., and Aretxabaleta, A. L. (2014). Physical and biogeochemical controls on light attenuation in a eutrophic, back-barrier estuary. *Biogeoscience* 11, 7193–7205. doi: 10.5194/bg-11-7193-2014

Giri, C., Long, J., Abbas, S., Murali, R. M., Qamer, F. M., Pengra, B., et al. (2014). Distribution and dynamics of mangrove forests of South Asia. *J. Environ. Manage.* 148, 101–111. doi: 10.1016/j.jenvman.2014.01.020

Grasshoff, K. (1983). "Determination of salinity and oxygen; Determination of nutrients," in *Methods of Seawater Analysis*, eds K. Grasshoff, M. Ehrhard, and K. Kremling (New York, NY: Verlag Chemie), 31–125.

Hansell, D. A., and Carlson, C. A. (2001). Marine dissolved organic matter and the carbon cycle. *Oceanography* 14, 41–49. doi: 10.5670/oceanog.2001.05

Hansell, D. A., Carlson, C. A., Repeta, D. J., and Schlitzer, R. (2009). Dissolved organic matter in the ocean. *Oceanography* 22, 202–211.

Hansen, A. M., Kraus, T. E. C., Pellerin, B. A., Fleck, J. A., Downing, B. D., and Bergamaschi, B. A. (2016). Optical properties of dissolved organic matter (DOM): effects of biological and photolytic degradation. *Limnol. Oceanogr.* 61, 1015–1032. doi: 10.1002/lno.10270

Harvey, T. E., Ktatzer, S., and Anderson, A. (2015). Relationships between colored dissolved organic matter and dissolved organic carbon in different coastal gradients of the Baltic Sea. *Ambio* 44, 392–401. doi: 10.1007/s13280-015-0658-4

Hedges, J. I. (2002). *Biogeochemistry of Marine Dissolved Organic Matter*. San Diego: Academic Press, 1–33.

Helms, J. R., Stubbins, A., Perdue, M., Green, N. W., Chen, H., and Mopper, K. (2013). Photochemical bleaching of oceanic dissolved organic matter and its effect on absorption spectral slope and fluorescence. *Mar. Chem.* 155, 81–91. doi: 10.1016/j.marchem.2013.05.015

Helms, J. R., Stubbins, A., Ritchie, J. D., Minor, E. C., Kieber, D. J., and Mopper, K. (2008). Absorption spectral slopes and slope ratios as indicator of molecular weight, source, and photobleaching of chromophoric dissolved organic matter. *Limnol.Oceanogr.* 53, 955–969. doi: 10.4319/lo.2008.53.3.0955

Hernes, P. J., Benner, R., Cowie, G. L., Goñi, M., Bergamaschi, B., and Hedges, J. I. (2001). Tannin diagenesis in mangrove leaves from a tropical estuary: a novel molecular approach. *Geochim. Cosmochim. Acta* 65, 3109–3122. doi: 10.1016/s0016-7037(01)00641-x

Ho, D. T., Ferrón, S., Engel, V. C., Anderson, W. T., Swart, P. K., Price, R. M., et al. (2017). Dissolved carbon biogeochemistry and export in mangrove dominated rivers of the Florida Everglades. *Biogeosciences* 14, 2543–2559. doi: 10.5194/bg-14-2543-2017

IPCC (2007). *Climate Change 2007: The Physical Science Basis. Contribution of Working Group I to the Fourth Assessment Report of the Intergovernmental Panel on Climate Change*. Cambridge, MA: Cambridge University Press.

Jaffe, R., McKnight, D., Maie, N., Cory, R., McDowell, W. H., and Campbell, J. L. (2008). Spatial and temporal variations in DOM composition in ecosystems: the importance of long-term monitoring of optical properties. *J. Geophys. Res.* 113:G04032. doi: 10.1029/2008JG000683

Jennerjahn, T. C., and Ittekkot, V. (2002). Relevance of mangroves for the production and deposition of organic matter along tropical continental margins. *Naturwissenschaften* 89, 23–30. doi: 10.1007/s00114-001-0283-x

Kida, M., Tanabe, M., Tomotsune, M., Yoshitake, S., Kinjo, K., Ohtsuka, T., et al. (2019). Changes in dissolved organic matter composition and dynamics in a subtropical mangrove river driven by rainfall. *Estuar. Coast. Shelf Sci.* 223, 6–17. doi: 10.1016/j.ecss.2019.04.029

Kumar, M. D., Rajendran, A., Somasundar, K., Haake, B., Jenisch, A., Shuo, Z., et al. (1990). Dynamics of dissolved organic carbon in the northwestern Indian Ocean. *Mar. Chem.* 31, 299–316. doi: 10.1016/0304-4203(90)90044-d

Lønborg, C., and Álvarez-Salgado, X. A. (2012). Recycling versus export of bioavailable dissolved organic matter in the coastal ocean and efficiency of the continental shelf pump. *Glob. Biogeochem. Cycle* 26:GB3018. doi: 10.1029/2012GB004353

Lu, C.-H., Benner, R., Fichot, C. G., Fukuda, H., Yamashita, Y., and Ogawa, H. (2016). Sources and transformations of dissolved lignin phenols and chromophoric dissolved organic matter in Otsuchi Bay, Japan. *Front. Mar.Sci.* 3:85. doi: 10.3389/fmars.2016.00085

Maher, D. T., Santos, I. R., Golsby-Smith, L., Gleeson, J., and Eyre, B. D. (2013). Groundwater-derived dissolved inorganic and organic carbon exports from a mangrove tidal creek: the missing mangrove carbon sink? *Limnol. Oceanogr.* 58, 475–488. doi: 10.4319/lo.2013.58.2.0475

Maie, N., Pisani, O., and Jaffé, R. (2008). Mangrove tannins in aquatic ecosystems: their fate and possible influence on dissolved organic carbon and nitrogen. *Limnol. Oceanogr.* 53, 160–171. doi: 10.4319/lo.2008.53.1.0160

Maie, N., Yamashita, Y., Cory, R. M., Boyer, J. N., and Jaffé, R. (2012). Application of excitation emission matrix fluorescence monitoring in the assessment of spatial and seasonal drivers of dissolved organic matter composition: sources and physical disturbance controls. *Appl. Geochem.* 27, 917–929. doi: 10.1016/j.apgeochem.2011.12.021

Midorikawa, T., and Tanoue, E. (1998). Molecular masses and chromophoric properties of dissolved organic ligands for copper (II) in oceanic water. *Mar. Chem.* 62, 219–239. doi: 10.1016/s0304-4203(98)00040-1

Mitchell, B. G., Kahru, M., Wieland, J., and Stramska, M. (2003). "Determination of spectral absorption coefficients of particles, dissolved material and phytoplankton for discrete water samples," in *Ocean Optics Protocols for Satellite Ocean Color Sensor Validation, Revision 4. Volume IV, NASA/ TM-2003-211621*, eds J. L. Mueller, G. S. Fargion, and C. R. McClain (Greenbelt, MD: NASA Goddard Space Flight Center), 39–64.

Mukhopadhyay, S. K., Biswas, H., De, T. K., and Jana, T. K. (2006). Fluxes of nutrients from the tropical River Hooghly at the land–ocean boundary of Sundarbans, NE Coast of Bay of Bengal, India. *J. Marine Syst.* 62, 9–21. doi: 10.1016/j.jmarsys.2006.03.004

Nandi, T., Mandal, S., Deb, S., Ghosh, M., and Nath, T. (2018). Short-term variations in surface water properties in the Sundarban Estuarine System, India. *Sustain. Water Resour. Manag.* 4, 559–566. doi: 10.1007/s40899-017-0139-y

Ogawa, H., Amagai, Y., Koike, I., Kaiser, K., and Benner, R. (2001). Production of refractory dissolved organic matter by bacteria. *Science* 292, 917–920. doi: 10.1126/science.1057627

Osburn, C. L., Retamal, L., and Vincent, W. F. (2009). Photoreactivity of chromophoric dissolved organic matter transported by the Mackenzie River to the Beaufort Sea. *Mar. Chem.* 115, 10–20. doi: 10.1016/j.marchem.2009.05.003

Parvathy, K. G., and Bhaskaran, P. K. (2017). Wave attenuation in presence of mangroves: a sensitivity study for varying bottom slopes. *Inter. J. Ocean Clim. Syst.* 8, 126–134. doi: 10.1177/1759313117702919

Pelizzetti, E., and Calza, P. (2002). "Photochemical processes in the euphotic zone of Sea Water: progress and problems," in *Chemistry of Marine Water and Sediments. Environmental Science*, eds A. Gianguzza, E. Pelizzetti, and S. Sammartano (Berlin: Springer).

Peltier, W. R., Liu, Y., and Crowleay, J. W. (2007). Snowball Earth prevention by dissolved organic carbon remineralization. *Nature* 450, 813–819.

Ray, R., Baum, A., Gleixner, G., Rixen, T., and Jana, T. K. (2018a). Exportation of dissolved (inorganic and organic) and particulate carbon from mangroves and their implications to the carbon budget in the Indian Sundarbans. *Sci. Total Environ.* 621, 535–547. doi: 10.1016/j.scitotenv.2017.11.225

Ray, R., Ganguly, D., Chowdhury, C., Dey, M., Das, S., Dutta, M. K., et al. (2011). Carbon sequestration and annual increase of carbon stock in a mangrove forest. *Atmos. Environ.* 45, 5016–5024. doi: 10.1016/j.atmosenv.2011.04.074

Ray, R., Majumder, N., Chowdhury, C., Das, S., and Jana, T. K. (2017). Phosphorus budget of the Sundarban mangrove ecosystem: box model approach. *Estuar. Coast.* 41, 1036–1049. doi: 10.1007/s12237-017-0332-0

Ray, R., Majumder, N., Das, S., Chowdhury, C., and Jana, T. K. (2014). Biogeochemical cycle of nitrogen in a tropical mangrove ecosystem, east coast of India. *Mar. Chem.* 167, 33–43. doi: 10.1016/j.marchem.2014.04.007

Ray, R., Michaud, E., Aller, R. C., Vantrepotte, V., Gleixner, G., Walcker, R., et al. (2018b). Sources and distribution of carbon (DOC, POC, DIC) in a mangrove dominated estuary (French Guiana, South America). *Biogeochemistry* 138, 297–321. doi: 10.1007/s10533-018-0447-9

Ray, R., Rixen, T., Baum, A., Malik, A., Gleixner, G., and Jana, T. K. (2015). Distribution, sources and biogeochemistry of organic matter in a mangrove dominated estuarine system (Indian Sundarbans) during the pre-monsoon. *Estuar. Coast. Shelf Sci.* 167, 404–413. doi: 10.1016/j.ecss.2015.10.017

Ray, R., and Shahraki, M. (2016). Multiple sources driving the organic matter dynamics in two contrasting tropical mangroves. *Sci. Total Environ.* 571, 218–227. doi: 10.1016/j.scitotenv.2016.07.157

Raymond, P. A., and Spencer, R. G. M. (2013). "Riverine DOM," in *Book Biogeochemistry of Marine Dissolved Organic Matter*, 2nd Edn, eds D. A. Hansell and C. A. Carlson (Cambridge, MA: Academic Press), 509–533. doi: 10.1016/b978-0-12-405940-5.00011-x

Romera-Castillo, C., and Jaffé, R. (2015). Free radical scavenging (antioxidant activity) of natural dissolved organic matter. *Mar. Chem.* 177, 668–676. doi: 10.1016/j.marchem.2015.10.008

Roshith, C. M., Meena, D. K., Manna, R. K., Sahoo, A. K., Swain, H. S., Raman, R. K., et al. (2018). Phytoplankton community structure of the Gangetic (Hooghly-Matla) estuary: status and ecological implications in relation to eco-climatic variability. *Flora* 240, 133–143. doi: 10.1016/j.flora.2018.01.001

Rudra, K. (2014). Changing river courses in the western part of the Ganga-Brahmaputra delta. *Geomorphology* 227, 87–100. doi: 10.1016/j.geomorph.2014.05.013

Sadat-Noori, M., Maher, D. T., and Santos, I. R. (2016). Groundwater Discharge as a Source of Dissolved Carbon and Greenhouse Gases in a Subtropical Estuary. *Estuar. Coast.* 39, 639–656. doi: 10.1007/s12237-015-0042-4

Samanta, S., Dalai, T. K., Pattanaik, J. K., Rai, S. K., and Mazumdar, A. (2015). Dissolved inorganic carbon (DIC) and its δ13C in the Ganga (Hooghly) River estuary, India: evidence of DIC generation via organic carbon degradation and carbonate dissolution. *Geochim. Cosmochim. Acta* 165, 226–248. doi: 10.1016/j.gca.2015.05.040

Samanta, S., Dalai, T. K., Tiwari, S. K., and Rai, S. K. (2018). Quantification of source contributions to the water budgets of the Ganga (Hooghly) River estuary, India. *Mar. Chem.* 207, 42–54. doi: 10.1016/j.marchem.2018.10.005

Santos, I. R., Maher, D. T., and Eyre, B. D. (2012). Coupling automated radon and carbon dioxide measurements in coastal waters. *Environ. Sci Technol.* 46, 7685–7691. doi: 10.1021/es301961b

Santos, L., Pinto, A., Filipe, O., Cunha, Â, Santos, E. B. H., and Almeida, A. (2016). Insights on the optical properties of Estuarine DOM – hydrological and biological influences. *PLoS One* 11:e0154519. doi: 10.1371/journal.pone.0154519

Sanyal, P. (1983). Mangrove tiger land, the Sundarbans of India. *Tigerpaper* 10, 1–4.

Sarkar, S. S., Mondal, P., Biswas, J. K., Kwon, E. E., SikOk, Y., and Rinklebe, J. (2017). Trace elements in surface sediments of the Hooghly (Ganges) estuary: distribution and contamination risk assessment. *Environ. Geochem. Health* 39, 1245–1258. doi: 10.1007/s10653-017-9952-3

Sarmiento, J. L., and Gruber, N. (2006). *Ocean Biogeochemical Dynamics*. Princeton, NJ: Princeton University Press.

Scheibe, A., Krantz, L., and Gleixner, G. (2012). Simultaneous determination of the quantity and isotopic signature of dissolved organic matter from soil water using highperformance liquid chromatography/isotope ratio mass spectrometry. *Rapid Commun. Mass Sp.* 26, 173–180. doi: 10.1002/rcm.5311

Schwartz, J. N., Kowalczuk, P., Kaczmerak, S., Cota, G. F., Mitchell, B. G., and Kahru, M. (2002). Two models for absorption by coloured dissolved organic matter (CDOM). *Oceanologia* 44, 209–241.

Scully, N. M., Maie, N., Dailey, S. K., Boyer, J. N., Jones, R. D., and Jaffé, R. (2004). Early diagenesis of plant-derived dissolved organic matter along a wetland, mangrove, estuary ecotone. *Limnol. Oceanogr.* 49, 1667–1678. doi: 10.4319/lo.2004.49.5.1667

Seitzinger, S. P., Harrison, J. A., Dumont, E., Beusen, A. H. W., and Bouwman, A. F. (2005). Sources and delivery of carbon, nitrogen, and phosphorus to the coastal zone: an overview of Global Nutrient Export from Watersheds (NEWS) models and their application. *Glob. Biogeochem. Cycles* 19:GB4S01. doi: 10.1029/2005GB002606

Shah, C., Sudheer, A. K., and Bhusan, R. (2018). Distribution of dissolved organic carbon in the Bay of Bengal: influence of sediment discharge, freshwater flux, and productivity. *Mar. Chem.* 203, 91–101. doi: 10.1016/j.marchem.2018.04.004

Shank, G. C., Lee, R., Vähätalo, A., Zepp, R. G., and Bartels, E. (2010). Production of chromophoric dissolved organic matter from mangrove leaf litter and floating Sargassum colonies. *Mar. Chem.* 119, 172–181. doi: 10.1016/j.marchem.2010.02.002

Shank, G. C., Nelson, K., and Montagna, K. (2009). Importance of CDOM distribution and photo reactivity in a shallow Texas Estuary. *Estur. Coasts* 32, 661–677. doi: 10.1007/s12237-009-9159-7

Sholkovitz, E. R. (1976). Flocculation of dissolved organic and inorganic matter during the mixing of river water and seawater. *Geochim. Cosmochim. Acta* 40, 831–845. doi: 10.1016/0016-7037(76)90035-1

Sippo, J. Z., Maher, D. T., Tait, D. R., Ruiz-Halpern, S., Sanders, C. J., and Santos, I. R. (2017). Mangrove outwelling is a significant source of oceanic exchangeable organic carbon. *Limnol. Oceanogr. Lett.* 2, 1–8. doi: 10.1002/lol2.10031

Spencer, R. G. M., Aiken, G. R., Dornblaser, M. M., Butler, K. D., Holmes, R. M., Fiske, G., et al. (2013). Chromophoric dissolved organic matter export from U.S. rivers. *Geophys. Res. Lett.* 40, 1575–1579. doi: 10.1002/grl.50357

Spencer, R. G. M., Butler, K. D., and Aiken, G. R. (2012). Dissolved organic carbon and chromophoric dissolved organic matter properties of rivers in the USA. *J. Geophys. Res. Biogeosci.* 117:G03001. doi: 10.1029/2011JG001928

Spencer, R. G. M., Hernes, P. J., Ruf, R., Baker, A., Dyda, R. Y., Stubbins, A., et al. (2010). Temporal controls on dissolved organic matter and lignin biogeochemistry in a pristine tropical river, Democratic Republic of Congo. *J. Geophys. Res. Biogeosci.* 115:G03013. doi: 10.1029/2009JG001180

Spencer, R. G. M., Stubbins, A., Hernes, P. J., Baker, A., Mopper, K., and Aufdenkampe, A. K. (2009). Photochemical degradation of dissolved organic matter and dissolved lignin phenols from the Congo River. *J. Geophys. Res.* 114:G03010. doi: 10.1029/2009JG000968

Stedmon, C. A., Amon, R. M. W., Rinehart, A. J., and Walker, S. A. (2011). The supply and characteristics of colored dissolved organic matter (CDOM) in the Arctic Ocean: pan arctic trends and differences. *Mar. Chem.* 124, 108–118. doi: 10.1016/j.marchem.2010.12.007

Strickland, J. D. H., and Parsons, T. R. (1972). *A Practical Handbook of Seawater Analysis*, 2nd Edn. Canada: Bull. Fisheries Res. Board.

Thurman, E. M. (1985). *Organic Geochemistry of Natural Waters*. Dordrecht: Nijhoff/Junk.

Twilley, R. R. (1985). The exchange of organic carbon in basin mangrove forests in a southwestern Florida estuary. *Estuar. Coast. Shelf Sci.* 20, 543–557. doi: 10.1016/0272-7714(85)90106-4

Tzortziou, M., Osburn, C. L., and Neale, P. J. (2007). Photobleaching of dissolved organic material from a tidal marsh-estuarine system of the Chesapeake Bay. *Photochem. Photobiol.* 83, 782–792. doi: 10.1111/j.1751-1097.2007.00142.x

Vähätalo, A., Søndergaard, M., Schlüter, L., and Markager, S. (1998). The impact of solar radiation on the decomposition of detrital leaves of eelgrass (*Zostera marina*). *Mar. Ecol. Prog. Ser.* 170, 107–117. doi: 10.3354/meps170107

Vantrepotte, V., Danhiez, F. P., Loisel, H., Ouillon, S., Mériaux, X., Cauvin, A., et al. (2015). CDOM-DOC relationship in contrasted coastal waters: implication for DOC retrieval from ocean color remote sensing observation. *Opt. Express* 23, 33–54.

Vodacek, A., Blough, N. V., Degrandpre, M. D., Peltzer, E. T., and Nelson, R. K. (1997). Seasonal variation of CDOM and DOC in the Middle Atlantic Bight: terrestrial inputs and photooxidation. *Limnol. Oceanogr.* 42, 674–686. doi: 10.4319/lo.1997.42.4.0674

Weishaar, J., Aiken, G., Bergamaschi, B., Fram, M., Fugii, R., and Mopper, K. (2003). Evaluation of specific ultraviolet absorbance as an indicator of the chemical composition and reactivity of dissolved organic carbon. *Environ. Sci. Technol.* 37, 4702–4708. doi: 10.1021/es030360x

Yamashita, Y., Nosaka, Y., Suzuki, K., Ogawa, H., Takahashi, K., and Saito, H. (2013). Photobleaching as a factor controlling spectral characteristics of chromophoric dissolved organic matter in open ocean. *Biogeoscience* 10, 7207–7217. doi: 10.5194/bg-10-7207-2013

Yamashita, Y., and Tanoue, E. (2009). Basin scale distribution of chromophoric dissolved organic matter in the Pacific Ocean. *Limnol. Oceanogr.* 54, 598–609. doi: 10.4319/lo.2009.54.2.0598

Yang, L., Hong, H., Chen, C.-T. A., Guo, W., and Huang, T.-H. (2013). Chromophoric dissolved organic matter in the estuaries of populated and mountainous Taiwan. *Mar. Chem.* 157, 12–23. doi: 10.1016/j.marchem.2013.07.002

Zhang, J., Zhao, J., Yang, G., and Liu, W. (2019). Concentration and characterization of colored dissolved organic matter in the surface microlayer and subsurface water of the yellow Sea and the East China Sea. *J. Ocean Univ. China* 18, 383–393. doi: 10.1007/s11802-019-3763-3

Zweifel, U. L., Wikner, J., Hagstrom, A., Lundberg, E., and Norrman, B. (1995). Dynamics of dissolved organic carbon in a coastal ecosystem. *Limnol. Oceanogr.* 40, 299–305. doi: 10.4319/lo.1995.40.2.0299

Conflict of Interest: The authors declare that the research was conducted in the absence of any commercial or financial relationships that could be construed as a potential conflict of interest.